Stimulation of BM cells with an endotoxin, lipopolysaccharide (LPS), for 5 h *ex vivo*, increased the amount of not only IL-6 but also TNFα to levels significantly higher in *Rx291/Ezh2*$^{\Delta/\Delta}$ BM cells compared with *Rx291* BM cells (Fig. 5e). In addition, Rx291/Ezh2$^{\Delta/\Delta}$ mice at the MDS stage showed significantly elevated levels of circulating IL-6 protein in the PB serum (Fig. 5f). These findings indicate that *Rx291/Ezh2*$^{\Delta/\Delta}$-MDS cells, despite their compromised proliferative capacity, outcompete WT HSPCs by impeding their function via an inflammation-related mechanism in the MDS BM environment.

RUNX1S291fs helps PRC1 repress *Hoxa9* in the absence of Ezh2. MDS patients with *EZH2* mutations show low risk of transformation to AML and *EZH2* mutations are rare in *de novo* AML[2]. Indeed, none of the Rx291/Ezh2$^{\Delta/\Delta}$ mice developed typical *de novo* AML in this study. We therefore examined expression of target genes of *MLL-AF9* and *NUP98-HOXA9* fusions[44,45] in LSK cells by GSEA, and found that *Rx291/Ezh2*$^{\Delta/\Delta}$-MDS LSK cells had negative enrichment of canonical AML target genes (Table 2 and Supplementary Fig. 7). Among these AML target genes, *Hoxa9* is critical for both HSCs and *MLL-AF9*-positive AML cells[44,46].

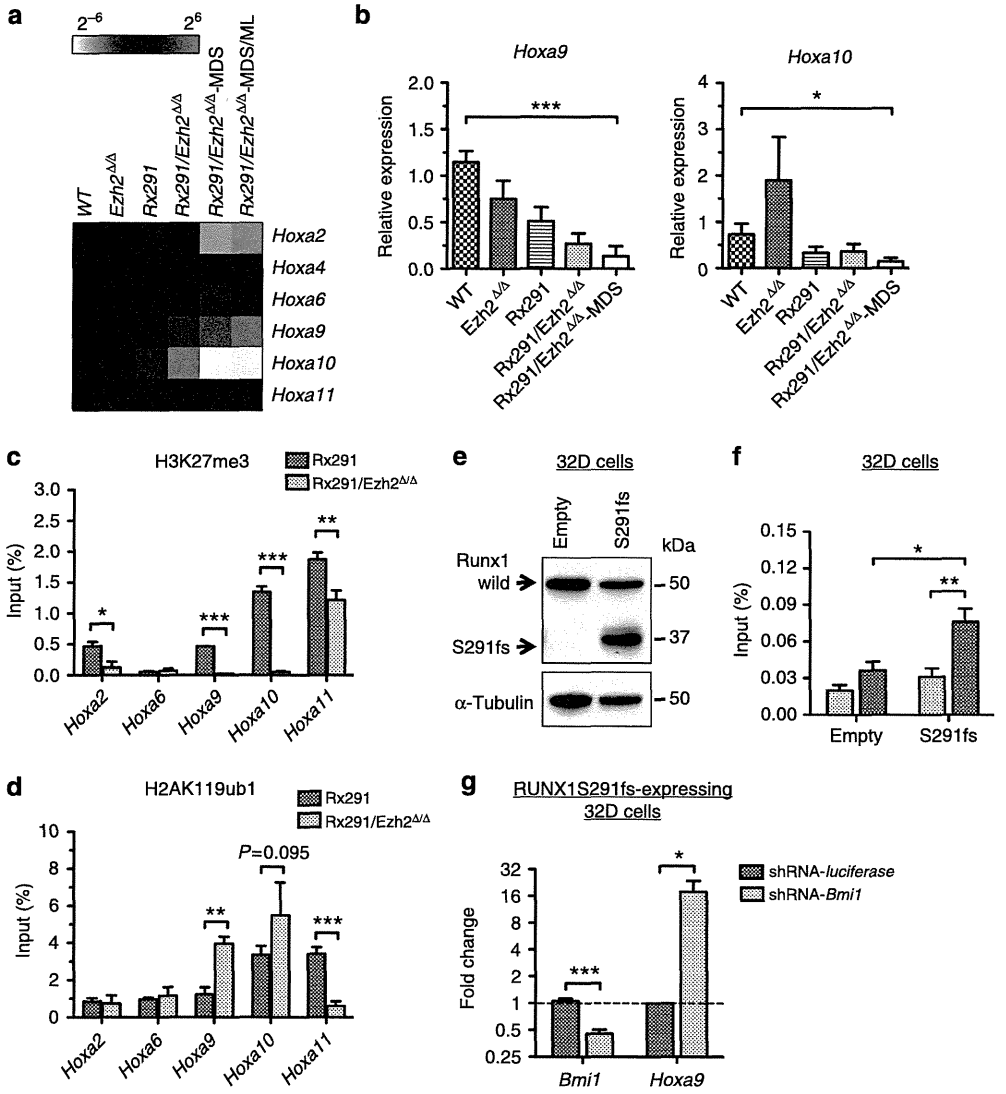

Figure 6 | RUNX1S291fs helps PRC1 repress *Hoxa9* expression in the absence of Ezh2. (**a**) Heat map showing expression profiles of *Hoxa* genes in CD45.2$^+$GFP$^+$ LSK cells from WT, Ezh2$^{\Delta/\Delta}$, Rx291 and Rx291/Ezh2$^{\Delta/\Delta}$ mice at 4 months post transplantation (pre-MDS stage) and from moribund Rx291/Ezh2$^{\Delta/\Delta}$-MDS and MDS/ML mice. (**b**) Quantitative RT-PCR analysis of the expression of *Hoxa9* and *Hoxa10* in LSK cells from WT, Ezh2$^{\Delta/\Delta}$, Rx291 and Rx291/Ezh2$^{\Delta/\Delta}$ mice at 4 months post transplantation (pre-MDS stage) and from moribund Rx291/Ezh2$^{\Delta/\Delta}$-MDS mice ($n=4$–5). Scale bars and asterisk show mean ± s.d., $^*P<0.05$ and $^{***}P<0.001$ by Student's *t*-test. (**c**,**d**) Levels of H3K27me3 (**c**) and H2AK119ub1 (**d**) at the promoters of *Hoxa* genes in *Rx291* and *Rx291/Ezh2*$^{\Delta/\Delta}$ LSK cells as detected by ChIP-QPCR. The relative amounts of immunoprecipitated DNA are depicted as a percentage of input DNA. Scale bars and asterisks show mean ± s.e.m., $^*P<0.05$, $^{**}P<0.01$ and $^{***}P<0.001$ by Student's *t*-test ($n=4$). (**e**) Detection of RUNX1S291fs protein in *RUNX1S291fs*-expressing 32D cells by western blotting using an anti-RUNX1 antibody. α-Tubulin was detected as a loading control. Arrows indicate endogenous Runx1 and RUNX1S291fs proteins. (**f**) Recruitment of Bmi1 to the *Hoxa9* promoter in *RUNX1S291fs*-expressing 32D cells. Localization of Bmi1 at the *Hox9a* promoter was evaluated in 32D cells and *RUNX1S291fs*-expressing 32D cells by ChIP-QPCR. The relative amounts of immunoprecipitated DNA are depicted as a percentage of input DNA. Scale bars and asterisks show means ± s.e.m., $^*P<0.05$ and $^{**}P<0.01$ by Student's *t*-test ($n=3$). (**g**) Derepression of *Hoxa9* by knockdown of *Bmi1* detected by quantitative RT-PCR. 32D cells expressing RUNX1S291fs were infected with lentiviruses expressing shRNA directed to a *Luciferase* control or *Bmi1*. Scale bars and asterisk show mean ± s.e.m., $^*P<0.05$ and $^{***}P<0.001$ by Student's *t*-test ($n=4$).

© 2014 Macmillan Publishers Limited. All rights reserved.

Expression of *Hoxa9* was downregulated in LSK cells expressing RUNX1S291fs mutant and further depressed by *Ezh2* loss at the MDS stage (Fig. 6a). RT–PCR confirmed that expression of *Hoxa9* as well as that of *Hoxa10*, another oncogene characteristic of AML, was significantly downregulated in *Rx291/Ezh2*$^{\Delta/\Delta}$-MDS LSK cells compared with WT LSK cells (Fig. 6b).

In contrast to *Mecom/Evi1*, promoter DNA hypermethylation was not involved in the repression of *Hoxa9* expression in *Rx291/Ezh2*$^{\Delta/\Delta}$ LSK cells (Supplementary Fig. 8). We and other group recently reported that RUNX1 recruit PRC1 via direct binding to Bmi1 to establish transcriptional repression of genes in a context-dependent manner[12,47]. We therefore hypothesized that the RUNX1S291fs mutant might collaborate with Bmi1 to suppress expression of *Hoxa9*. We first performed a chromatin immunoprecipitation (ChIP)–QPCR assay for H3K27me3 and H2AK119ub1 at promoters of the *Hoxa* gene cluster using *Rx291* and *Rx291/Ezh2*$^{\Delta/\Delta}$ LSK cells. We found that levels of H3K27me3 were markedly reduced at *Hoxa9* and *Hoxa10* promoters in *Rx291/Ezh2*$^{\Delta/\Delta}$ cells (Fig. 6c). By contrast, H2AK119ub1 was significantly enriched at the *Hoxa9* promoter in *Rx291/Ezh2*$^{\Delta/\Delta}$cells compared with *Rx291* cells (Fig. 6d). To determine whether Bmi1 binds to the promoter region of *Hoxa9*, we performed a ChIP–QPCR assay using an anti-Bmi1 antibody in murine 32D cells expressing RUNX1S291fs (Fig. 6e) due to the paucity of primary LSK cells. As expected, Bmi1 significantly bound to the *Hoxa9* promoter in RUNX1S291fs-expressing 32D cells compared with the control 32D cells (Fig. 6f). To determine whether the recruitment of Bmi1 contributed to transcriptional repression of *Hoxa9*, we transduced short hairpin RNA (shRNA) directed to *Bmi1* or *luciferase*, a negative control, in *RUNX1S291fs*-expressing 32D cells. Knockdown of *Bmi1* induced a significant elevation of *Hoxa9* expression in *RUNX1S291fs*-expressing 32D cells (Fig. 6g). We also observed that RUNX1S291fs mutant physically associates with Bmi1 in RUNX1S291fs-expressing 32D cells (Supplementary Fig. 9). Taken together, the RUNX1S291fs mutant promotes PRC1-mediated transcriptional repression of *Hoxa9* in the absence of Ezh2. While Ezh2 loss alone did not significantly affect the levels of H3K27me3 at the promoter of *Hoxa9*, it induced a mild increase in the levels of H2AK119ub1 and moderately repressed the expression of *Hoxa9* (Fig. 6b and Supplementary Fig. 10). These findings imply that Ezh2 loss could also lead to the transcriptional repression of *Hoxa9*, although the underlying mechanism is obscure.

Inactivation of *Hoxa9* restrains MDS from leukaemic formation. We next interrogated the pathophysiological relevance of reduced *Hoxa9* expression to MDS. We first examined expression of *HOXA9* in CD34$^+$ stem/progenitor cells isolated from RCMD (refractory cytopenia with multilineage dysplasia), RAEBI/II (refractory anaemia with excess blasts I/II), MDS/AML, *de novo* AML patients and healthy volunteers by quantitative RT–PCR. While the level of *HOXA9* expression in MDS–RCMD and *de novo* AML patients was comparable to the control CD34$^+$ cells, it was significantly elevated to the levels higher than those of *MLL-AF9*-positive AML cell lines in both MDS–RAEBI/II and MDS/AML patients (Fig. 7a). Thus, *HOXA9* expression is robustly activated in high-risk MDS and MDS/AML patients, suggesting that the level of *HOXA9* expression is critical to the leukaemic transformation of MDS.

To test this hypothesis, we transduced ectopic *Hoxa9* into HSCs from WT and Rx291/Ezh2$^{\Delta/\Delta}$ mice. To evaluate the proliferative capacity of *Hoxa9*-expressing *Rx291/Ezh2*$^{\Delta/\Delta}$ HSCs, we first conducted serial replating assays *in vitro*. While *Rx291/Ezh2*$^{\Delta/\Delta}$cells did not form colonies after the second plating, *Hoxa9*-expressing *Rx291/Ezh2*$^{\Delta/\Delta}$cells acquired the capability to give rise to colonies and efficiently generated colonies even after the fourth replating, similar to *Hoxa9*-expressing WT cells (Figs 7b,c). We next transplanted *Hoxa9*-expressing HSCs into lethally irradiated recipient mice together with life-saving 2×10^5 BM cells. Notably, two out of four recipients transplanted with *Hoxa9*-expressing *Rx291/Ezh2*$^{\Delta/\Delta}$ cells developed AML with increased myeloblast cells (Fig. 7d), and died by 6 months post transplantation, while *Hoxa9*-expressing WT cells developed neither MPN nor AML within the observation period, possibly due to a longer latency[48]. *Hoxa9*-expressing *Rx291/Ezh2*$^{\Delta/\Delta}$ AML cells in the BM highly expressed both Mac1 and c-Kit antigens (Fig. 7e), similar to *MLL-AF9*-induced AML cells[15]. This phenotype was clearly distinct from *Rx291/Ezh2*$^{\Delta/\Delta}$-MDS cells in the BM (Fig. 7e). Taken together, the repressed *Hoxa9* expression inhibits the leukaemic transformation of *Rx291/Ezh2*$^{\Delta/\Delta}$-MDS cells.

Discussion

Our studies show that the loss of Ezh2 promotes initiation and propagation of RUNX1 mutant-induced MDS, which supports a tumour-suppressive role for *EZH2* in MDS. Our mouse model with concurrent *Ezh2* loss and *RUNX1S291fs* expression developed MDS-like features such as anaemia, leukopenia, impaired myeloid cells differentiation and multilineage dysplasia. In addition, our mouse model showed an obvious resistance to transform into AML as reported that a few *de novo* AML patients show mutations of *EZH2* (refs 1,2,18). Indeed, our MDS mice showed a gene expression profile distinct from AML induced by *MLL-AF9* or *NUP98-HOXA9* (refs 44,45). Interestingly, expression of *Hoxa9*, one of the most well-known leukaemic oncogenes, was dramatically repressed in our MDS mice in contrast to AML. It has been reported that *Hoxa9* deficiency impairs the proliferative capacity of HSCs, delays myeloid cell differentiation and decreases neutrophil counts[46], a phenotype that is quite similar to the ineffective hematopoiesis observed in *Rx291/Ezh2*$^{\Delta/\Delta}$-MDS mice, except for the dysplasia we observed. Although it remains unknown how downregulation of *Hoxa9* contributes to the development of MDS, we found that level of *HOXA9* expression in human CD34$^+$ cells was clearly correlated with the disease progression of MDS in patients. Given that AML transformation was induced by the ectopic expression of *Hoxa9* in *Rx291/Ezh2*$^{\Delta/\Delta}$ cells, we propose that the resistance to AML transformation in the absence of Ezh2 is at least in part dependent on the repression of *Hoxa9* expression. Another prototypical HSC regulator that has also been shown to drive leukaemia is *MECOM/EVI1* (ref. 39). In line with our observations in this study, however, expression of *EVI1* is generally low in MDS patients[47]. Downregulation of *Mecom/Evi1* expression may also contribute to the resistance to AML transformation in the absence of Ezh2. These findings indicate that our mouse model utilizing *Ezh2* loss and the *RUNX1S291fs* mutant accurately recapitulates many aspects of MDS harbouring *EZH2* mutations.

In MDS patients, mutant cells propagate in the BM despite impaired proliferative capacity and are thought to eventually outcompete normal hematopoietic cells[35]. Our findings in Rx291/Ezh2$^{\Delta/\Delta}$-MDS mice provided a clue to understand the mechanism of clonal competition between MDS clones and normal cells in MDS patients. *Rx291/Ezh2*$^{\Delta/\Delta}$-MDS cells appeared to be defective in proliferative capacity as evidenced by the reduced expression of two potent leukaemic oncogenes, *Hoxa9* and *Mecom/Evi1*. Of interest, inflammatory cytokine pathways such as IL-6 pathway, which are inhibitory towards HSCs[42] were significantly activated in residing normal HSPCs,

© 2014 Macmillan Publishers Limited. All rights reserved.

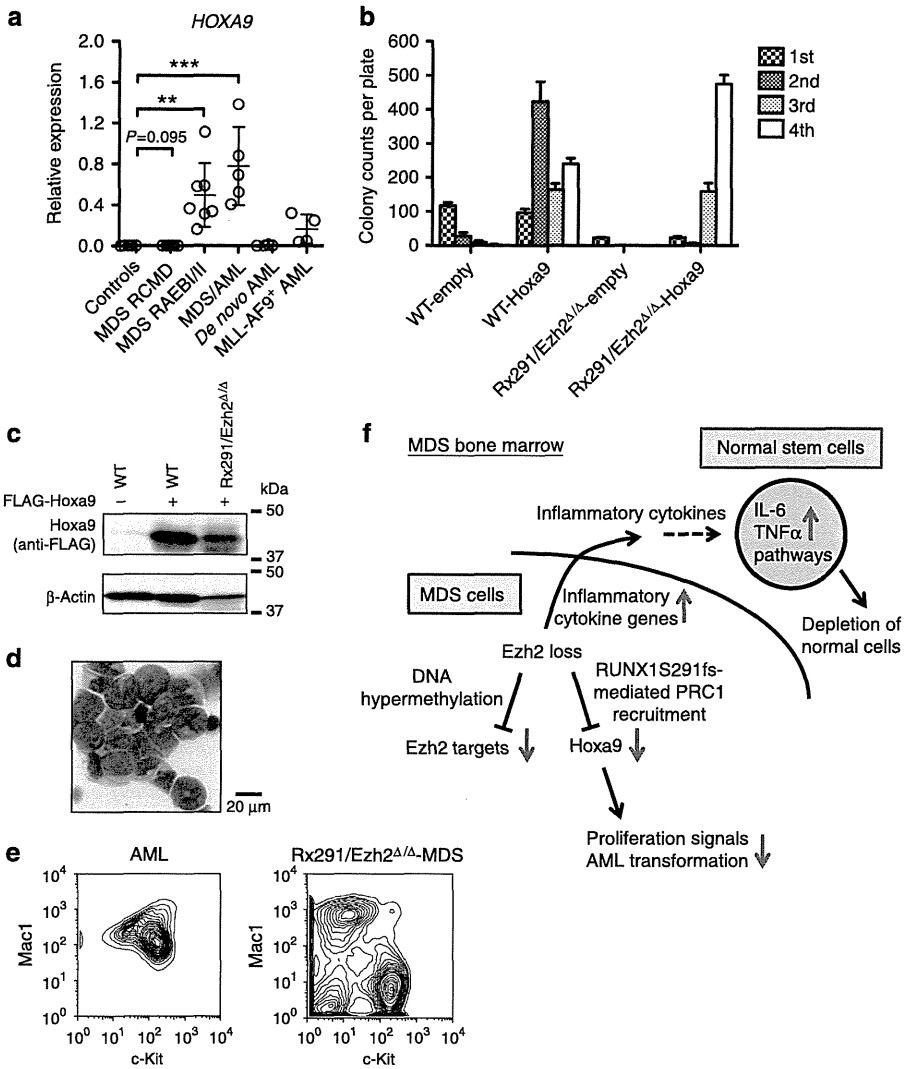

Figure 7 | *Hoxa9* expression level is critical for transformation from MDS to AML. (**a**) Quantitative RT-PCR analysis of the expression of *HOXA9* in CD34$^+$ cells of seven MDS-RCMD, seven MDS-RAEBI/II, five MDS/AML, four *de novo* AML patients, four *MLL-AF9*-positive AML cell lines (THP-1, NOMO-1, MOLM-13 and MONO-MAC1) and six healthy controls. Scale bars and asterisks show mean ± s.d., $^{**}P<0.01$, and $^{***}P<0.001$ by Mann-Whitney *U*-test. (**b**,**c**) Clonogenic capacity of *Rx291/Ezh2*$^{\Delta/\Delta}$cells overexpressing *Hoxa9*. WT and *Rx291/Ezh2*$^{\Delta/\Delta}$HSCs were transduced with a *Hoxa9* retrovirus and plated in methylcellulose media, then replated into the same medium every 14 days. The data are shown as mean ± s.e.m. ($n=3$) in **b**. Expression of exogenous Flag-tagged Hoxa9 protein in colony cells was detected by western blotting using an anti-Flag antibody in **c**. β-Actin was detected as a loading control. (**d**) Morphology of AML cells from BM of recipients infused with *Hoxa9*-expressing *Rx291/Ezh2*$^{\Delta/\Delta}$ cells observed by May-Grüenwald Giemsa staining. Scale bar, 20 μm. (**e**) Fluorescence-activated cell sorting profiles of BM cells from mouse in **d** and Rx291/Ezh2$^{\Delta/\Delta}$-MDS mouse. (**f**) A proposed model of the role of Ezh2 loss in the development of *RUNX1S291fs*-induced MDS.

but not in *Rx291/Ezh2*$^{\Delta/\Delta}$-mutant HSPCs in the same Rx291/Ezh2$^{\Delta/\Delta}$ mice. Indeed, expression of IL-6 was significantly elevated in *Rx291/Ezh2*$^{\Delta/\Delta}$ BM cells compared with *Rx291* BM cells at the level of both transcript and protein. *Rx291/Ezh2*$^{\Delta/\Delta}$ BM cells exhibited heightened sensitivity to LPS stimulation, and the level of circulating IL-6 protein in the PB serum was significantly elevated in Rx291/Ezh2$^{\Delta/\Delta}$ mice during the development of MDS. Excessive IL-6 production by MDS cells has also been shown to promote leukopenia and thrombocytosis through the activation of Traf6 in a 5q-MDS mouse model[49]. In addition, combined exposure of IL-6, CCL2 and TNFα has been reported to impair normal HSC function *in vivo* and inhibition of these cytokines rescues the impaired HSC function[43]. Recent studies indicated that CML cells alter the BM microenvironment to impair normal HSCs, but favour CML stem cells function, at least in part, via activation of inflammatory cytokines[29,30]. All these findings support that activation of inflammatory cytokine responses largely accounts for compromised normal hematopoiesis in our MDS model. In our model, *Rx291/Ezh2*$^{\Delta/\Delta}$-MDS cells outcompete normal cells by activating inflammatory responses, thereby achieving clonal expansion despite their compromised proliferative capacity (Fig. 7f). Our findings provide additional evidence of non-autonomous cells mechanisms that promote the expansion of MDS clones in the MDS BM environment.

Since Ezh2 functions to repress transcription via H3K27me3 modification, its absence could lead to the activation of its target genes[7]. However, we observed that Ezh2 target genes were mostly kept transcriptionally repressed in *Rx291/Ezh2*$^{\Delta/\Delta}$ HSPCs at the MDS stage. We have recently shown that *Tet2*$^{KD/KD}$*Ezh2*$^{\Delta/\Delta}$MDS LSK cells maintain the transcriptional repression of Ezh2 targets via the complementary function of Ezh1 (ref. 20). Similarly, we observed residual enrichments of H3K27me3 at specific genes (for example, *Hoxa11*), so the same mechanism may also operate

© 2014 Macmillan Publishers Limited. All rights reserved.

in *RUNX1S291fs/Ezh2*-null MDS cells. In this study, however, we identified two alternative epigenetic mechanisms underlying the repression of Ezh2 targets in *RUNX1S291fs*-expressing cells (Fig. 7f). First, *Rx291/Ezh2*$^{\Delta/\Delta}$ HSPCs showed promoter DNA hypermethylation at some Ezh2 target genes, and this appeared to repress expression of important developmental regulator genes of both hematopoietic and non-hematopoietic lineages (for example, *Mecom/Evi1*, *Pdx1* and *Hand1*). As described above, expression of *MECOM/EVI1* is generally low in MDS patients and its upregulation may trigger leukaemic transformation[24,47] Our findings raise the possibility that promoter DNA hypermethylation is a major molecular mechanism that keeps *MECOM/EVI1* transcriptionally repressed in MDS patients. Second, we found that expression of *Hoxa9* was repressed through RUNX1S291fs-directed PRC1 recruitment in the absence of Ezh2. Importantly, *HOXA9* expression is closely repressed in MDS–RCMD patients irrespective of the *RUNX1* mutations. Given that repression of *Hoxa9* is critical to attenuate the predisposition of MDS to develop into AML, there are presumably several different ways to establish repression of *Hoxa9*, and it would be intriguing to address this issue. Nonetheless, the repressed *Hoxa9* expression appears to be a hallmark of MDS-specific epigenetic alteration.

In conclusion, our findings provide a comprehensive picture of how Ezh2 loss functions to collaborate with RUNX1 mutant in the pathogenesis of MDS in both cell autonomous and non-autonomous manners, and how it attenuates the predisposition of MDS clones to transform into AML. While many studies have demonstrated that EZH2 functions as an oncogene in various tumours, we have experimentally demonstrated the tumour-suppressive function of EZH2 in MDS *in vivo*. Since there are only a few mouse models available for human MDS[34], we hope that this MDS model will contribute to our understanding of the role of altered epigenetic regulations in the pathogenesis of MDS and to the innovation of novel therapies for MDS.

Methods

Mice. *Ezh2* conditional knockout (*Ezh2*$^{flox/flox}$) mice were previously described, and crossed with *Rosa26-Cre-ERT* mice for conditional deletion[32]. C57BL/6 mice congenic for the Ly5 locus (CD45.1) were purchased from Sankyo-Lab Service. All experiments using the mice were performed in accordance with our institutional guidelines for the use of laboratory animals and approved by the Review Board for animal experiments of Chiba University (approval ID: 25-104) or Cincinnati Children's Hospital Medical Center.

Retroviral transduction and transplantation. *pMYs-empty control-IRES-GFP*, *pMYs-RUNX1S291fs-IRES-GFP* and *pMYs-RUNX1D171N-IRES-GFP* vectors were previously described[24]. *CS-H1-shRNA-EF-1α-EGFP* vector expressing shRNA-directed *Bmi1* or *luciferase* were previously described[50]. *Hoxa9* cDNA was kindly provided by Dr Takuro Nakamura, and the cDNA was subcloned into pMYs vector. Retrovirus infection into CD34$^-$LSK HSCs was performed as previously described[51]. Briefly, retrovirus-infected 50 HSCs were cultured in SF-O3 medium containing 50 ng ml^{-1} mouse SCF and 50 ng ml^{-1} human TPO for 3 days, and then these HSCs were intravenously injected in 8.5 Gy or 9 Gy irradiated CD45.1$^+$ mice together with radioprotective 2×10^5 CD45.1$^+$ BM cells. At 6 weeks post transplantation, 1 mg tamoxifen was administered via intraperitoneal injection for 5 consecutive days to completely delete *Ezh2* alleles[32].

Colony assay. Colony assays were performed in Methocult M3234 (Stem Cell Technologies) supplemented with 20 ng ml^{-1} mouse SCF, 20 ng ml^{-1} mouse IL-3, 20 ng ml^{-1} human TPO and 2 units ml^{-1} human EPO. The number of colonies was counted at day14 of culture. For replating assay, colonies were scored at day14 and pooled 3×10^4 cells were replated into the same medium.

Cell culture. BM cells were stimulated with or without 10 ng ml^{-1} LPS (*Escherichia coli* 0127:B8; Sigma-Aldrich) in 10% fetal bovine serum RPMI supplemented with 10 ng ml^{-1} mouse IL-3 and GolgiStop (BD 554724) containing monensin, which inhibits intracellular protein transport processes.

Flow cytometry and antibodies. Flow cytometry and cell sorting were performed by utilizing the following monoclonal antibodies; CD45.2 (104), CD45.1 (A20), Gr1 (RB6-8C5), CD11b/Mac1 (M1/70), Ter119, CD71 (R17217), CD127/IL-7Rα (A7R34), B220 (RA3-6B2), CD4 (L3T4), CD8α (53-6.7), CD117/c-Kit (2B8), Sca1 (D7), CD34 (MEC14.7) and FcγRII-III (93)[32]. These antibodies were purchased from eBioscience or BioLegend. Lineage mixture solution contains Gr1, Mac1, B220, CD4, CD8α, Ter119 and IL-7Rα biotin-conjugated antibodies. Apoptotic cells were stained with anti-Annexin V-APC antibody (BD 550474) and with propidium iodide following staining cell surface markers to discriminate Lineage$^-$Sca1$^+$c-Kit$^+$ cells or CD71$^+$Ter119$^+$ cells. To evaluate cellular proliferation, cells were fixed and permeabilized (FIX & PERM, Invitrogen) according to the manufacturer's instruction, and then detected by using anti-Ki67-PE antibody (BD 556027) following staining cells by lineage mixture, streptavidin-APC-Cy7, Sca1 PE-Cy7 and c-Kit APC antibodies. To evaluate intracellular amounts of IL-6 and TNFα proteins, BM cells were fixed and permeabilized and then detected by using anti-IL-6 (BD 554401) and anti-TNFα (BD 557730) antibodies following staining cells with CD45.2 antibody. All flow cytometry analyses and cell sorting were performed on FACSAriaII or FACSCantoII (BD).

Quantitative RT-PCR. Quantitative RT–PCR was performed on a StepOnePlus Real time PCR System (Life Technologies) by using SYBR Premix Ex TaqII (Takara) or FastStart Universal Probe Master (Roche) with a Universal Probe Library (Roche) and primers shown in Supplementary Table 4. The expression levels of *HOXA9* and *GAPDH* were examined by using TaqMan Gene Expression Assays (Hs03929097_g1 and Hs00266821_m1, respectively; Life Technologies). All data are presented as relative expression levels normalized to either *Gapdh or GAPDH* expression.

Microarray analysis. Total RNA was extracted from $\sim 2 \times 10^5$ pooled BM LSK cells (isolated from two to four mice per each genotype except diseased mouse) by using an RNeasy Plus Mini Kit (Qiagen). A quantity of 20 ng of total RNA was mixed with spike-in controls using an Agilent One Colour Spike Mix Kit (Agilent), amplified and labelled with Cyanine 3 using a Low Input Quick Amp Labeling Kit (Agilent) according to the manufacturer's instructions. Microarray analysis using a SurePrint G3 Mouse GE Microarray 8 × 60 K kit (Agilent) was performed according to the manufacturer's instructions. The raw data were deposited in Gene Expression Omnibus under the accession number GSE50537.

Western blotting ChIP and quantitative RT-PCR. Antibodies for western blotting and immunoprecipitation were as follows: anti-H3 (Abcam, ab1791), anti-H3K27me3 (Millipore 07449), anti-Bmi1 (clone 8A9, kindly provided by Dr N. Nozaki, MAB Institute), anit-RUNX1 (Abcam, ab23980), anti-FLAG (M2, Sigma), anti-β-Actin (Santa Cruz, sc-47778), and anti-α-Tubulin (Santa Cruz, sc-5286). Uncropped raw scans of blots used in the figures are presented in Supplementary Fig. 11. ChIP assays were performed as previously described[15]. Briefly, 1×10^5 pooled BM LSK cells were used for each immunoprecipitation. The following antibodies were used for the immunoprecipitation reactions: anti-H3K27me3 (Millipore 07449), anti-H2AK119ub1 (Cell Signaling, 8240), anti-Bmi1 (Bethyl A301694A) and pre-immune immunoglobulin G. DNA was amplified by quantitative RT–PCR on a StepOnePlus Real time PCR System (Life Technologies) using primers shown in Supplementary Table 4.

Cytokine assay. Amounts of mouse IL-6 in PB serum were measured by ELISA kit (BD Bioscience) according to the manufacturer's protocol.

RRBS. Total 500 ng genomic DNA extracted from LSK cells (isolated from two to three mice per each genotype and a disease mouse) were digested with MspI restriction enzyme that recognizes and cleaves CCGG tetranucleotide sequences irrespective of their methylation. DNA fragments were then subjected to end-repair and dA-tailing using an NEBNext DNA Library Prep Master Mix Set (NEB, Ipswich, MA), followed by the ligation with methylated adaptor oligo-DNA (Illumina, San Diego, CA). After the bisulphite conversion from unmethylated cytosine to uracil by using an EZ DNA Methylation kit (Zymo Research, Irvine, CA) followed by agarose gel excision of fragments ranging from 150 bp to 400 bp, DNA fragments ligated with adaptors in both ends were amplified by 18 cycles of PCR using PE1.0 and PE2.0 oligo primers (Illumina). The generated library was sequenced by the 36 bp single-end protocol of GAIIx (Illumina) using two lanes of a flow cell. As unmethylated cytosine of the library is converted to thymine during the PCR amplification, mapping of sequenced tags to murine reference genome (mm9, UCSC Genome Browser) was performed by Bismark software[52], which can align bisulphite-converted tags to genome and evaluate their methylation simultaneously. In this study, methylation level was estimated in CpGs with ≥10 reads (713,353 CpGs per sample in an average). Statistical analysis was done by methyl kit[53]. As promoters were defined as regions spanning −2.5 to +0.5 Kb from transcription start sites and containing ≥5 CpGs that can be evaluated as ≥10 reads, these promoter regions were taken into account for differential methylation analysis. The raw data were deposited in DDBJ under the accession numbers, DRA001143, DRA001144, DRA001145 and DRA001146.

© 2014 Macmillan Publishers Limited. All rights reserved.

MDS patient samples. This study comprises MDS-RCMD ($n=7$), MDS-RAEBI/II ($n=7$), MDS/AML ($n=5$) and *de novo* AML ($n=4$) patients at the Hiroshima University Hospital. CD34$^+$ blood cells were isolated using a CD34 MicroBead kit and autoMACS system (Milteny Biotec, Germany). Patient anonymity was ensured, and the study was approved by the Institutional Review Committee at Hiroshima University. Patients gave written informed consent for the study according to the Declaration of Helsinki.

References

1. Bejar, R. *et al.* Clinical effect of point mutations in myelodysplastic syndromes. *N. Engl. J. Med.* **364,** 2496–2506 (2011).
2. Shih, A. H., Abdel-Wahab, O., Patel, J. P. & Levine, R. L. The role of mutations in epigenetic regulators in myeloid malignancies. *Nat. Rev. Cancer* **12,** 599–612 (2012).
3. Chung, Y. R., Schatoff, E. & Abdel-Wahab, O. Epigenetic alterations in hematopoietic malignancies. *Int. J. Hematol.* **96,** 413–427 (2012).
4. Sashida, G. & Iwama, A. Epigenetic regulation of hematopoiesis. *Int. J. Hematol.* **96,** 405–412 (2012).
5. Sauvageau, M. & Sauvageau, G. Polycomb group proteins: multi-faceted regulators of somatic stem cells and cancer. *Cell Stem Cell* **7,** 299–313 (2010).
6. Wang, H. *et al.* Role of histone H2A ubiquitination in Polycomb silencing. *Nature* **431,** 873–878 (2004).
7. Cao, R. *et al.* Role of histone H3 lysine 27 methylation in Polycomb-group silencing. *Science* **298,** 1039–1043 (2002).
8. Boyer, L. a. *et al.* Polycomb complexes repress developmental regulators in murine embryonic stem cells. *Nature* **441,** 349–353 (2006).
9. Francis, N. J., Kingston, R. E. & Woodcock, C. L. Chromatin compaction by a polycomb group protein complex. *Science* **306,** 1574–1577 (2004).
10. Tavares, L. *et al.* RYBP-PRC1 complexes mediate H2A ubiquitylation at polycomb target sites independently of PRC2 and H3K27me3. *Cell* **148,** 664–678 (2012).
11. Simon, J. a. & Kingston, R. E. Occupying chromatin: polycomb mechanisms for getting to genomic targets, stopping transcriptional traffic, and staying put. *Mol. Cell* **49,** 808–824 (2013).
12. Yu, M. *et al.* Direct recruitment of Polycomb repressive complex 1 to chromatin by core binding transcription factors. *Mol. Cell* **45,** 330–343 (2012).
13. Morin, R. D. *et al.* Somatic mutations altering EZH2 (Tyr641) in follicular and diffuse large B-cell lymphomas of germinal-center origin. *Nat. Genet.* **42,** 181–185 (2010).
14. Herrera-Merchan, A. *et al.* Ectopic expression of the histone methyltransferase Ezh2 in haematopoietic stem cells causes myeloproliferative disease. *Nat. Commun.* **3,** 623 (2012).
15. Tanaka, S. *et al.* Ezh2 augments leukemogenicity by reinforcing differentiation blockage in acute myeloid leukemia. *Blood* **120,** 1107–1117 (2012).
16. Ernst, T. *et al.* Inactivating mutations of the histone methyltransferase gene EZH2 in myeloid disorders. *Nat. Genet.* **42,** 722–726 (2010).
17. Nikoloski, G. *et al.* Somatic mutations of the histone methyltransferase gene EZH2 in myelodysplastic syndromes. *Nat. Genet.* **42,** 665–667 (2010).
18. Bejar, R. *et al.* Validation of a prognostic model and the impact of mutations in patients with lower-risk myelodysplastic syndromes. *J. Clin. Oncol.* **30,** 3376–3382 (2012).
19. Jerez, A. *et al.* Loss of heterozygosity in 7q myeloid disorders: clinical associations and genomic pathogenesis. *Blood* **119,** 6109–6117 (2012).
20. Muto, T. *et al.* Concurrent loss of Ezh2 and Tet2 cooperates in the pathogenesis of myelodysplastic disorders. *J. Exp. Med.* **210,** 2627–2639 (2013).
21. Niimi, H. *et al.* Hyperactivation of the RAS signaling pathway in myelodysplastic syndrome with AML1/RUNX1 point mutations. *Leukemia.* **20,** 635–644 (2006).
22. Harada, H. *et al.* High incidence of somatic mutations in the AML1/RUNX1 gene in myelodysplastic syndrome and low blast percentage myeloid leukemia with myelodysplasia. *Blood* **103,** 2316–2324 (2004).
23. Papaemmanuil, E. *et al.* Clinical and biological implications of driver mutations in myelodysplastic syndromes. *Blood* **122,** 3616–3627 (2013).
24. Watanabe-Okochi, N. *et al.* AML1 mutations induced MDS and MDS/AML in a mouse BMT model. *Blood* **111,** 4297–4308 (2008).
25. Sawada, K. *et al.* Proliferation and differentiation of myelodysplastic CD34+ cells: phenotypic subpopulations of marrow CD34+ cells. *Blood* **85,** 194–202 (1995).
26. Passegué, E., Jamieson, C. H. M., Ailles, L. E. & Weissman, I. L. Normal and leukemic hematopoiesis: are leukemias a stem cell disorder or a reacquisition of stem cell characteristics? *Proc. Natl Acad. Sci. USA* **100** (suppl.), 11842–11849 (2003).
27. Walkley, C. R. *et al.* A microenvironment-induced myeloproliferative syndrome caused by retinoic acid receptor gamma deficiency. *Cell* **129,** 1097–1110 (2007).
28. Raaijmakers, M. H. G. P. *et al.* Bone progenitor dysfunction induces myelodysplasia and secondary leukaemia. *Nature* **464,** 852–857 (2010).
29. Zhang, B. *et al.* Altered microenvironmental regulation of leukemic and normal stem cells in chronic myelogenous leukemia. *Cancer Cell* **21,** 577–592 (2012).
30. Schepers, K. *et al.* Myeloproliferative neoplasia remodels the endosteal bone marrow niche into a self-reinforcing leukemic niche. *Cell Stem Cell* **13,** 285–299 (2013).
31. Su, I. *et al.* Polycomb group protein ezh2 controls actin polymerization and cell signaling. *Cell* **121,** 425–436 (2005).
32. Mochizuki-Kashio, M. *et al.* Dependency on the polycomb gene Ezh2 distinguishes fetal from adult hematopoietic stem cells. *Blood* **118,** 6553–6561 (2011).
33. Kogan, S. C. *et al.* Bethesda proposals for classification of nonlymphoid hematopoietic neoplasms in mice. *Blood* **100,** 238–245 (2002).
34. Nimer, S. D. MDS: a stem cell disorder--but what exactly is wrong with the primitive hematopoietic cells in this disease? *Hematology.* **2008,** 43–51 (2008).
35. Raza, A. & Galili, N. The genetic basis of phenotypic heterogeneity in myelodysplastic syndromes. *Nat. Rev. Cancer* **12,** 849–859 (2012).
36. Abdel-Wahab, O. *et al.* Deletion of Asxl1 results in myelodysplasia and severe developmental defects *in vivo*. *J. Exp. Med.* **210,** 2641–2659 (2013).
37. Shen, X. *et al.* EZH1 mediates methylation on histone H3 lysine 27 and complements EZH2 in maintaining stem cell identity and executing pluripotency. *Mol. Cell* **32,** 491–502 (2008).
38. Chambers, S. M. *et al.* Hematopoietic fingerprints: an expression database of stem cells and their progeny. *Cell Stem Cell* **1,** 578–591 (2007).
39. Goyama, S. & Kurokawa, M. Evi-1 as a critical regulator of leukemic cells. *Int. J. Hematol.* **91,** 753–757 (2010).
40. Herman, J. G. & Baylin, S. B. Gene silencing in cancer in association with promoter hypermethylation. *N. Engl. J. Med.* **349,** 2042–2054 (2003).
41. Essers, M. a. G. *et al.* IFNalpha activates dormant haematopoietic stem cells *in vivo*. *Nature* **458,** 904–908 (2009).
42. King, K. Y. & Goodell, M. a. Inflammatory modulation of HSCs: viewing the HSC as a foundation for the immune response. *Nat. Rev. Immunol.* **11,** 685–692 (2011).
43. Chen, C., Liu, Y., Liu, Y. & Zheng, P. Mammalian target of rapamycin activation underlies HSC defects in autoimmune disease and inflammation in mice. *J. Clin. Invest.* **120,** 4091–4101 (2010).
44. Krivtsov, A. V. *et al.* Transformation from committed progenitor to leukaemia stem cell initiated by MLL-AF9. *Nature* **442,** 818–822 (2006).
45. Takeda, A., Goolsby, C. & Yaseen, N. R. NUP98-HOXA9 induces long-term proliferation and blocks differentiation of primary human CD34+ hematopoietic cells. *Cancer Res.* **66,** 6628–6637 (2006).
46. Lawrence, H. J. *et al.* Loss of expression of the Hoxa-9 homeobox gene impairs the proliferation and repopulating ability of hematopoietic stem cells. *Blood* **106,** 3988–3994 (2005).
47. Harada, Y. *et al.* RUNX1/AML1 mutant collaborates with BMI1 overexpression in the development of human and murine myelodysplastic syndromes. *Blood* **121,** 3434–3446 (2013).
48. Thorsteinsdottir, U. *et al.* Overexpression of the myeloid leukemia-associated Hoxa9 gene in bone marrow cells induces stem cell expansion. *Blood* **99,** 121–129 (2002).
49. Starczynowski, D. T. *et al.* Identification of miR-145 and miR-146a as mediators of the 5q- syndrome phenotype. *Nat. Med.* **16,** 49–58 (2010).
50. Chiba, T. *et al.* Enhanced self-renewal capability in hepatic stem/progenitor cells drives cancer initiation. *Gastroenterology* **133,** 937–950 (2007).
51. Konuma, T. *et al.* Forced expression of the histone demethylase Fbxl10 maintains self-renewing hematopoietic stem cells. *Exp. Hematol.* **39,** 697–709 (2011).
52. Krueger, F. & Andrews, S. R. Bismark: a flexible aligner and methylation caller for Bisulfite-Seq applications. *Bioinformatics.* **27,** 1571–1572 (2011).
53. Akalin, A. *et al.* methylKit: a comprehensive R package for the analysis of genome-wide DNA methylation profiles. *Genome Biol.* **13,** R87 (2012).
54. Dasu, M. R. K., Hawkins, H. K., Barrow, R. E., Xue, H. & Herndon, D. N. Gene expression profiles from hypertrophic scar fibroblasts before and after IL-6 stimulation. *J. Pathol.* **202,** 476–485 (2004).

Acknowledgements

We thank Dr Jun Matsubayashi for suggestions in histological analysis and members of the Iwama Laboratory for discussion during the preparation of this manuscript. This work was supported in part by Grants-in-aid for Scientific Research (#23591367, #24249054, #25130702) and Scientific Research on Innovative Areas 'Cell Fate' (#22118004) from MEXT, Japan, a Grant-in-aid for Core Research for Evolutional Science and Technology (CREST) from the Japan Science and Technology Corporation (JST) and grants from the Takeda Science Foundation, the Uehara Memorial Foundation and the Kanae Foundation.

Author contributions

G.S. designed the research, performed experiments, analysed results and wrote the manuscript; H.H., H.M. and Y.H. performed experiments and analysed results; M.Y., S.T., A.S. and Y.H. performed experiments; M.O., M.M.-K., C.W., T.M., K.S., H.N., T.I., G.H. and T.K. assisted in the experiments; H. K. provided mice; and A.I. designed the research, analysed results and wrote the manuscript.

© 2014 Macmillan Publishers Limited. All rights reserved.

Additional information

Accession codes: The microarray data has been deposited in the Gene Expression Omnibus under accession code GSE50537. The bisulphite sequencing data have been deposited in the DDBJ under the accession codes DRA001143, DRA001144, DRA001145 and DRA001146.

Supplementary Information accompanies this paper at http://www.nature.com/naturecommunications

Competing financial interests: The authors declare no competing financial interests.

Reprints and permission information is available online at http://npg.nature.com/reprintsandpermissions/

How to cite this article: Sashida, G. *et al.* Ezh2 loss promotes development of myelodysplastic syndrome but attenuates its predisposition to leukaemic transformation. *Nat. Commun.* 5:4177 doi: 10.1038/ncomms5177 (2014).

© 2014 Macmillan Publishers Limited. All rights reserved.

Molecular and Virological Evidence of Viral Activation From Chromosomally Integrated Human Herpesvirus 6A in a Patient With X-Linked Severe Combined Immunodeficiency

Akifumi Endo,[1,2] Ken Watanabe,[3] Tamae Ohye,[4] Kyoko Suzuki,[5] Tomoyo Matsubara,[5] Norio Shimizu,[3] Hiroki Kurahashi,[4] Tetsushi Yoshikawa,[6] Harutaka Katano,[7] Naoki Inoue,[8] Kohsuke Imai,[1] Masatoshi Takagi,[1] Tomohiro Morio,[1] and Shuki Mizutani[1]

[1]Department of Pediatrics and Developmental Biology, Tokyo Medical and Dental University, [2]Department of Pediatrics, Tokyo Metropolitan Cancer and Infectious Diseases Center, Komagome Hospital, and [3]Department of Virology, Tokyo Medical and Dental University, [4]Division of Molecular Genetics, Fujita Health University, Toyoake; [5]Department of Pediatrics, Juntendo University Urayasu Hospital, [6]Department of Pediatrics, Fujita Health University, Toyoake, Departments of [7]Pathology and [8]Virology I, National Institute of Infectious Diseases, Tokyo, Japan

(See the Editorial Commentary by Flamand on pages 549–51.)

It has been unclear whether chromosomally integrated human herpesvirus 6 (ciHHV-6) can be activated with pathogenic effects on the human body. We present molecular and virological evidence of ciHHV-6A activation in a patient with X-linked severe combined immunodeficiency. These findings have significant implications for the management of patients with ciHHV-6.

Keywords. ciHHV-6; HHV-6; X-SCID; hemophagocytic syndrome; thrombotic microangiopathy.

Human herpesvirus 6 (HHV-6) is a ubiquitous DNA virus that is the causative agent of roseola infantum, and infects individuals by 3 years of age [1]. After primary infection, HHV-6 establishes a latent state in the host. There are 2 distinct species, HHV-6A and HHV-6B. Most HHV-6 infections are caused by HHV-6B, whereas HHV-6A is less common. Chromosomally integrated HHV-6 (ciHHV-6) is the state in which HHV-6 (HHV-6A or HHV-6B) is integrated into the host germline genome, and it is transmitted vertically in a Mendelian manner. Although ciHHV-6 affects about 1% of the general population, it is generally considered to be a nonpathogenic condition. However, it is unclear whether ciHHV-6 can be activated with pathogenic effects on the human body [2].

Severe combined immunodeficiency (SCID) is a group of genetic disorders that result in a combined absence of T- and B-cell immunity. It is characterized by life-threatening infections during the first year of life unless treated, usually with hematopoietic stem cell transplantation (HSCT). X-linked severe combined immunodeficiency (X-SCID) arises from a mutation in the interleukin 2 receptor, gamma (*IL2RG*) gene on the X-chromosome [3]. We encountered a boy with X-SCID in whom ciHHV-6A was activated.

CASE REPORT

A 2-month-old boy was hospitalized for recurrent episodes of fever, cough, diarrhea, and failure to thrive. Upon admission, a viral infection was suspected, and supportive care did not improve his symptoms.

Twenty days after admission, mild pancytopenia (leukocyte count, 1.4×10^9/L; hemoglobin level, 78 g/L; and platelet count, 37×10^9/L) and elevated aminotransferases and ferritin were evident (aspartate aminotransferase, 448 U/L; alanine aminotransferase, 218 U/L; and ferritin, 4325 ng/mL) (Supplementary Figure 1). A bone marrow biopsy showed a hypocellular condition without dysplastic changes, as well as increased activated phagocytes. These results suggested hemophagocytic syndrome (HPS).

An immunological evaluation revealed an absence of T cells and low immunoglobulin levels. Genetic analysis identified a mutation in the *IL2RG* that was consistent with X-SCID. The patient's mother was heterozygous for the same mutation, and there was no such mutation detected in the patient's father.

A comprehensive search for a pathogen identified high levels of HHV-6 DNA (1.2×10^7 copies/μg DNA) in his peripheral blood. Antiviral treatment with ganciclovir or foscarnet did not reduce the viral load, and ciHHV-6 was suspected. We detected high levels of HHV-6 DNA in the patient's fingernails, the father's peripheral blood, and the father's hair follicles (5.9×10^5, 1.0×10^7, 1.2×10^6 copies/μgDNA, respectively).

Received 7 January 2014; accepted 9 April 2014; electronically published 6 May 2014.
Correspondence: Shuki Mizutani, MD, Department of Pediatrics and Developmental Biology, Tokyo Medical and Dental University, 1-5-45, Yushima, Bunkyo-ku, Tokyo 113-8510, Japan (skkmiz@gmail.com).

Clinical Infectious Diseases 2014;59(4):545–8
© The Author 2014. Published by Oxford University Press on behalf of the Infectious Diseases Society of America. All rights reserved. For Permissions, please e-mail: journals.permissions@oup.com.
DOI: 10.1093/cid/ciu323

Downloaded from http://cid.oxfordjournals.org/ at University of Tokyo Library on April 24, 2015

Fluorescence in situ hybridization analysis of the patient's fibroblasts and his father's peripheral blood mononuclear cells (PBMCs) confirmed HHV-6 integration at chromosome 22 in both individuals (Figure 1); these results suggested vertical germline transmission.

However, discontinuation of antiviral treatment led to a deterioration of the patient's HPS. Because no other pathogen was detected, activation of HHV-6 was suspected. To confirm this suspicion, we performed 3 assays that could detect viral activation despite the presence of integrated HHV-6 DNA. First, reverse transcription polymerase chain reaction (RT-PCR) was used to detect viral RNA in whole-blood samples. RT-PCR was performed on 2 HHV-6 genes, the late gene U60/66 and the immediate-early (IE) gene IE1, as described previously [5]. We detected viral RNA for both genes (4.6×10^2 copies/μg RNA for U60/66 and 5.2×10^3 copies/μg RNA for IE1). Second, immunostaining was used to detect IE antigens in a bone marrow sample taken at the time of HPS (Figure 2 and Supplementary Figure 2) [6]. Last, HHV-6A was isolated from the patient's PBMCs. It was cultured with cord blood cells and its presence confirmed by immunofluorescent staining with an anti–HHV-6 monoclonal antibody (Figure 3 and Supplementary Figure 3) [1].

Two hypotheses were postulated: Either the patient with ciHHV-6 was infected de novo with HHV-6, or HHV-6 was activated from the ciHHV-6 genome present in this patient. We performed a sequence analysis of the HHV-6 IE1 gene, as IE1 is variable and readily used to distinguish between HHV-6 variants [7]. DNA samples from isolated HHV-6A (described above), the patient's fingernails, his father's hair follicles, and laboratory strains U1102 and Z29 were amplified by PCR and sequenced. Because active HHV-6 is not present in the fingernails or hair follicles, we could amplify the original integrated HHV-6 strain from the genomes in these tissues. To our surprise, the sequences and subsequent phylogenetic analysis revealed that the isolated virus was identical to the original integrated HHV-6A strain present in both the patient and his father. Furthermore, this HHV-6A strain was unique in that it differed from all other HHV-6 strains analyzed (Supplementary Figure 4). These results suggested that the isolated HHV-6A strain originated from the activation of ciHHV-6A. Analysis of 3 other viral genes (gB, U94, and DR) confirmed these results [8, 9].

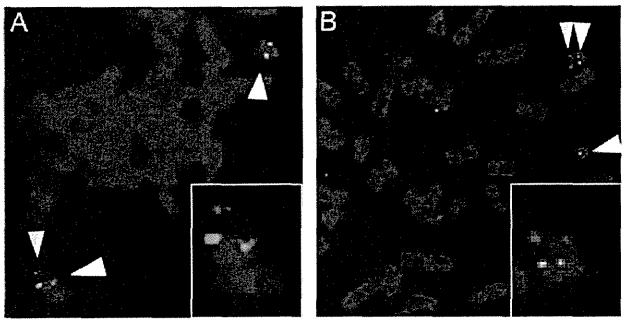

Figure 1. Integration of human herpesvirus type 6 (HHV-6) in chromosome 22 was demonstrated by fluorescence in situ hybridization analysis. Fibroblasts derived from the patient's skin (*A*) and peripheral blood mononuclear cells from the father (*B*) were cohybridized with HHV-6-specific (yellow arrow) and chromosome-22-specific probes (white arrows) [4]. HHV-6 integration in only one of the chromosome 22 alleles was shown in both materials. In sets of *A* and *B* are the enlared images of FISH data positively cohybridized with both probes.

The resumption of antiviral drug treatment with prednisolone ameliorated the patient's HPS. When he reached age 7 months, the patient underwent HSCT. Antiviral drug treatment was continued during HSCT, and engraftment was achieved 14 days after transplant. After engraftment, thrombotic microangiopathy (TMA) and gastrointestinal bleeding developed. Simultaneously, the patient's HHV-6A DNA and RNA titers increased, and HHV-6A was reisolated. Anticoagulant therapy and a reduction in tacrolimus dosage gradually improved the patient's TMA. With immunological reconstruction, the patient's HHV-6A DNA and RNA titers were successfully reduced and ultimately, no HHV-6A was isolated from subsequent blood samples. The asymptomatic patient was discharged at 12 months.

DISCUSSION

Since the discovery of ciHHV-6 in 1993, the question of whether ciHHV-6 can be activated from its integrated state has been perpetually debated [2]. With this case report, we provide the first molecular and virological evidence of viral activation from ciHHV-6A in the human body. This evidence comprises (1) viral RNA and antigens detected in PBMCs and bone marrow, as well as HHV-6A isolated from PBMCs; (2) HHV-6A sequences integrated into the patient's and his father's genomes, which were identical to those of the isolated virus; and (3) antiviral treatment and immunological reconstruction, which were effective in treating this activated ciHHV-6A.

In an effort to understand the biological significance of ciHHV-6, active viral replication from ciHHV-6 has recently been demonstrated in vitro under specific experimental conditions [9–11]. However, only a few studies have suggested ciHHV-6 activation in vivo despite high ciHHV-6 prevalence (approximately 1%) in the general population [12–14]. Activation of ciHHV-6 in vivo has been previously reported in mothers with ciHHV-6 who passed on the infection to infants who did not have inherited ciHHV-6 [8]. Our findings are consistent with these findings, as we clearly demonstrate the activation of HHV-6A in a patient who acquired ciHHV-6 via germline transmission.

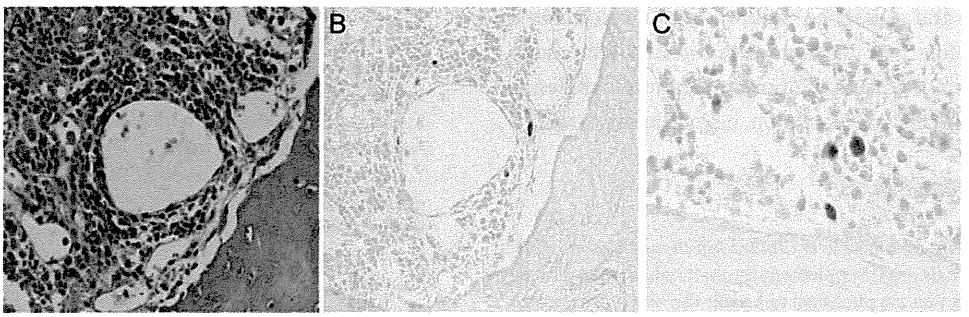

Figure 2. Histology and human herpesvirus type 6 (HHV-6) immunostaining. *A*, Hematoxylin and eosin staining of bone marrow. *B* and *C*, Immunostaining with an anti–HHV-6 antibody.

We speculate that the presence of X-SCID allowed for efficient activation of ciHHV-6A, and this phenomenon was detected with several technical strategies. Similarly, RT-PCR and virus isolation showed conversion from an HHV-6–positive status to a negative status with the patient's immunological recovery. In addition, these techniques were used to test samples taken from the patient's father. We were able to determine that he was indeed the ciHHV-6 carrier, yet he was HHV-6A negative. This suggests that X-SCID influenced the activation of ciHHV-6A. Because X-SCID prevalence is extremely low (about 0.001%), this case provides valuable insight into immunocompromised individuals and HHV-6 infection. However, the mechanism that triggered ciHHV-6A activation and replication in this patient remains to be elucidated. Further studies of patients with ciHHV-6 are required to determine what causes activation of this latent integrated virus.

The association between HHV-6 and HPS has previously been reported [15], and a link between HHV-6 and TMA has also been noted [16]. Therefore, it is possible that ciHHV-6A activation in our patient was associated with HPS and TMA. We noted that active HHV-6A infection coincided with symptom onset and the active infection was controlled with antiviral treatment. This suggests that HHV-6A is pathogenic, yet it remains to be established whether activated HHV-6A enhances underlying pathological conditions, and whether the activation of ciHHV-6A occurs in a similar fashion for all infected individuals.

Latent HHV-6 reactivation occurs in 40%–50% of recipients during HSCT, and our case report is the first to demonstrate that ciHHV-6A activation also occurs during this procedure. It is possible that the presence of X-SCID allowed for viral activation, but further studies are required to validate this hypothesis.

We have described the first case to provide molecular and virological evidence of the activation of chromosomally integrated HHV-6A in the human body. However, our report has limitations. We still do not know how virus production was triggered from a state of ciHHV-6A or how the production of the virus affected the patient's symptoms. Despite these limitations, based on this case, we hypothesize that an immunodeficient phenotype in conjunction with uncontrolled host defense systems allows the activation of ciHHV-6A. We support the recommendation that a screening program to detect ciHHV-6 in

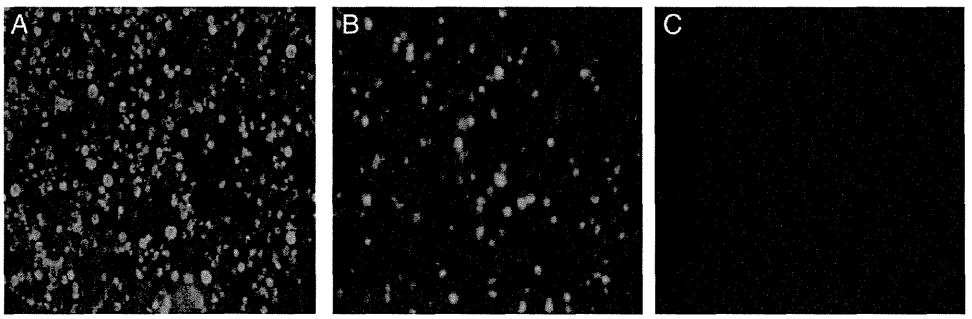

Figure 3. Immunofluorescent staining assay. *A*, Virus isolation confirmed with an anti– human herpesvirus type 6 antibody (gp116/64/54). *B*, U1102 cultured with cord blood cells (positive control). *C*, Cord blood cells alone (negative control).

Downloaded from http://cid.oxfordjournals.org/ at University of Tokyo Library on April 24, 2015

transplant patients and donors be established, and recommend that ciHHV-6 patients with immunocompromised status such as primary immunodeficiency, human immunodeficiency virus infection, or organ transplantation, be monitored carefully.

Supplementary Data

Supplementary materials are available at *Clinical Infectious Diseases* online (http://cid.oxfordjournals.org). Supplementary materials consist of data provided by the author that are published to benefit the reader. The posted materials are not copyedited. The contents of all supplementary data are the sole responsibility of the authors. Questions or messages regarding errors should be addressed to the author.

Notes

Financial support. This work was supported by the Ministry of Health, Labour, and Welfare of Japan (H25 Shinko-Ippan-015 to H. Ka., H23 Nanchi-Ippan-003 and H25 Nanchitou-Menneki-Ippan-105 to T. Mo.); the Japan Society for the Promotion of Science (22590426 to N. I.); and the Ministry of Education, Culture, Sciences, and Technology in Japan (23390270 and 23390271 to T. Mo. and S. M.).

Potential conflicts of interest. All authors: No reported conflicts.

All authors have submitted the ICMJE Form for Disclosure of Potential Conflicts of Interest. Conflicts that the editors consider relevant to the content of the manuscript have been disclosed.

References

1. Yamanishi K, Shiraki K, Kondo T, et al. Identification of human herpesvirus-6 as a causal agent for exanthema subitum. Lancet **1988**; 1: 1065–7.
2. Pellett PE, Ablashi DV, Ambros PF, et al. Chromosomally integrated human herpesvirus 6: questions and answers. Rev Med Virol **2012**; 22: 144–55.
3. Sugamura K, Asao H, Kondo M, et al. The interleukin-2 receptor gamma chain: its role in the multiple cytokine receptor complexes and T cell development in XSCID. Annu Rev Immunol **1996**; 14: 179–205.
4. Isegawa Y, Mukai T, Nakano K, et al. Comparison of the complete DNA sequences of human herpesvirus 6 variants A and B. J Virol **1999**; 73: 8053–63.
5. Van den Bosch G, Locatelli G, Geerts L, et al. Development of reverse transcriptase PCR assays for detection of active human herpesvirus 6 infection. J Clin Microbiol **2001**; 39:2308–10.
6. Papanikolaou E, Kouvatsis V, Dimitriadis G, Inoue N, Arsenakis M. Identification and characterization of the gene products of open reading frame U86/87 of human herpesvirus 6. Virus Res **2002**; 89:89–101.
7. Yamamoto T, Mukai T, Kondo K, Yamanishi K. Variation of DNA sequence in immediate-early gene of human herpesvirus 6 and variant identification by PCR. J Clin Microbiol **1994**; 32:473–6.
8. Gravel A, Hall CB, Flamand L. Sequence analysis of transplacentally acquired human herpesvirus 6 DNA is consistent with transmission of a chromosomally integrated reactivated virus. J Infect Dis **2013**; 207:1585–9.
9. Arbuckle JH, Medveczky MM, Luka J, et al. The latent human herpesvirus-6A genome specifically integrates in telomeres of human chromosomes in vivo and in vitro. Proc Natl Acad Sci U S A **2010**; 107:5563–8.
10. Prusty BK, Krohne G, Rudel T. Reactivation of chromosomally integrated human herpesvirus-6 by telomeric circle formation. PLoS Genet **2013**; 9:e1004033.
11. Huang Y, Hidalgo-Bravo A, Zhang E, et al. Human telomeres that carry an integrated copy of human herpesvirus 6 are often short and unstable, facilitating release of the viral genome from the chromosome. Nucleic Acids Res **2014**; 42:315–27.
12. Kobayashi D, Kogawa K, Imai K, et al. Quantitation of human herpesvirus-6 (HHV-6) DNA in a cord blood transplant recipient with chromosomal integration of HHV-6. Transpl Infect Dis **2011**; 13:650–3.
13. Troy SB, Blackburn BG, Yeom K, Caulfield AK, Bhangoo MS, Montoya JG. Severe encephalomyelitis in an immunocompetent adult with chromosomally integrated human herpesvirus 6 and clinical response to treatment with foscarnet plus ganciclovir. Clin Infect Dis **2008**; 47: e93–6.
14. Wittekindt B, Berger A, Porto L, et al. Human herpes virus-6 DNA in cerebrospinal fluid of children undergoing therapy for acute leukaemia. Br J Haematol **2009**; 145:542–5.
15. Tanaka H, Nishimura T, Hakui M, Sugimoto H, Tanaka-Taya K, Yamanishi K. Human herpesvirus-6-associated hemophagocytic syndrome in a healthy adult. Emerg Infect Dis **2002**; 8:87–8.
16. Matsuda Y, Hara J, Miyoshi H, et al. Thrombotic microangiopathy associated with reactivation of human herpesvirus-6 following high-dose chemotherapy with autologous bone marrow transplantation in young children thrombotic microangioapathy. Bone Marrow Transplant **1999**; 24:919–23.

Downloaded from http://cid.oxfordjournals.org/ at University of Tokyo Library on April 2, 2015

Bone Marrow Transplantation (2014) **49,** 1155–1161
© 2014 Macmillan Publishers Limited All rights reserved 0268-3369/14
www.nature.com/bmt

ORIGINAL ARTICLE

Cord blood transplantation is associated with rapid B-cell neogenesis compared with BM transplantation

K Nakatani[1], K Imai[2], M Shigeno[1], H Sato[3], M Tezuka[2], T Okawa[2], N Mitsuiki[1], T Isoda[2], D Tomizawa[2], M Takagi[2], M Nagasawa[2], M Kajiwara[4], M Yamamoto[5], A Arai[5], O Miura[5], C Kamae[6], N Nakagawa[6], K Honma[6], S Nonoyama[6], S Mizutani[1,2] and T Morio[1,2]

Hematopoietic cell transplantation (HCT) is used for treatment of hematopoietic diseases. Assessment of T- and B-cell reconstitution after HCT is crucial because poor immune recovery has a major effect on the clinical course. In this study, we retrospectively analyzed T-cell receptor excision circles (TRECs) as well as signal and coding joint kappa-deleting recombination excision circles (sjKRECs and cjKRECs, respectively) as markers of newly produced lymphocytes in 133 patients (56 primary immunodeficient and 77 malignant cases, median (range): 12 (0–62) years old). We analyzed the kinetics of TREC and KREC recovery and determined the factors that contributed to better immune recovery. KRECs became positive earlier than TRECs and increased thereafter. Younger recipient age had a favorable effect on recovery of sjKRECs and cjKRECs. Compared with BM and peripheral blood, our data suggested that cord blood (CB) provided rapid B-cell recovery. CB also provided better B-cell neogenesis in adult HCT recipients. Chronic GVHD was associated with low TRECs, but not increased sjKRECs/cjKRECs. Finally, positive sjKRECs 1 month after HCT were associated with fewer infectious episodes. Monitoring of TRECs and KRECs may serve as a useful tool for assessment of immune reconstitution post HCT.

Bone Marrow Transplantation (2014) **49,** 1155–1161; doi:10.1038/bmt.2014.123; published online 30 June 2014

INTRODUCTION

Hematopoietic cell transplantation (HCT) serves as a curative treatment for diseases such as hematopoietic malignancy, congenital BM failure and primary immunodeficiency (PID). Selection of a suitable donor by HLA matching and/or an appropriate conditioning regimen has improved the outcome of HCT for leukemia patients[1] and PID patients.[2,3] Recently, successful outcomes of cord blood transplantation (CBT) and BM transplantation (BMT) have been observed even in HLA-mismatched conditions.[4–8]

Despite these improved outcomes, transplantation-related morbidities such as graft failure, GVHD and infection are still major problems that affect the prognosis and/or quality of life. Infection monitoring after HCT is important for the initiation of preemptive therapy at the appropriate time, while assessment of immune reconstitution is essential because it is considered to be associated with post-transplant infection, relapse of primary disease and OS.[9]

CD4+ T-cell counts, T-cell proliferative capacity, B-cell number and serum IgG have been used as parameters of immune recovery after HCT. Recently, more direct assessment of T- and B-cell neogenesis has become feasible by analyses of T-cell receptor excision circles (TRECs) and kappa-deleting recombination excision circles (KRECs), respectively.

DNA fragments between rearranging V, D and J gene segments are deleted as circular excision products during rearrangement of the T-cell receptor gene.[10] These products are called TRECs. Quantitative detection of TRECs enables direct measurement of thymic output. The recovery of TRECs is associated with survival and infection after HCT for treatment of malignancies.[11–13] In a previous study, TREC levels were lower in patients post CBT than in those receiving BMT or PBSC transplantation (PBSCT).[14]

KRECs are formed by Ig kappa-deleting rearrangement during B-cell development. Coding joint KRECs (cjKRECs) serve as an indicator of B-cell numbers,[15] and signal joint KRECs (sjKRECs) are an indicator of B-cell neogenesis. However, the kinetics of KREC recovery post HCT are largely unknown. A correlation between KRECs and survival or infection after HCT has not been reported previously. In addition, whether B-cell recovery as assessed by KRECs is different among graft sources is still unknown.

Here, we investigated the kinetics of TREC and KREC recovery post HCT and factors contributing to better recovery of TREC and KREC levels, mainly focusing on KRECs. We also assessed the association of KRECs with infection after HCT in patients with malignancies or PID.

MATERIALS AND METHODS

Patients

A total of 133 patients who underwent allogeneic HCT from March 1996 to August 2013 were enrolled in this study. The patients were followed up at the Department of Pediatrics or Department of Hematology at Tokyo Medical and Dental University or the Department of Pediatrics of the National Defense Medical College in Japan. The median age at transplantation was 12 years (range, 0–62 years). Table 1 shows the patient characteristics, information on HCT and events associated with transplantation. This study was approved by the ethics committees of

[1]Department of Pediatrics and Developmental Biology, Tokyo Medical and Dental University Graduate School of Medical and Dental Sciences, Tokyo, Japan; [2]Department of Pediatrics, Tokyo Medical and Dental University Medical Hospital, Tokyo, Japan; [3]Department of Preventive Medicine and Public Health, National Defense Medical College, Saitama, Japan; [4]Department of Blood Transfusion, Tokyo Medical and Dental University Medical Hospital, Tokyo, Japan; [5]Department of Hematology, Tokyo Medical and Dental University Medical Hospital, Tokyo, Japan and [6]Department of Pediatrics, National Defense Medical College, Saitama, Japan. Correspondence: Dr T Morio, Department of Pediatrics and Developmental Biology, Tokyo Medical and Dental University Graduate School of Medical and Dental Sciences, 1-5-45 Yushima, Bunkyo-ku, Tokyo 113-8519, Japan. E-mail: tmorio.ped@tmd.ac.jp
Received 17 July 2013; revised 29 April 2014; accepted 1 May 2014; published online 30 June 2014

Table 1. Patient characteristics and clinical course

	PID (56)	*Malignancy (77)*	*All (133)*
Patient characteristics			
Recipient age			
< 18 years	45	44	89
⩾ 18 years	11	33	44
Sex			
Male	42	44	86
Female	14	33	47
Conditioning			
RIC or minimal conditioning	33	10	43
MA	23	66	89
Donor age (BM)			
< 18 years	5	8	13
⩾ 18 years	25	38	63
Cell source			
BM	35	47	82
CB	19	17	36
PB	2	13	15
HLA allele			
⩽ 5/6	20	31	51
6/6	23	33	56
Relation			
Related	13	30	43
Unrelated	43	47	90
Steroid use	28 (52%)	32 (42%)	60 (46%)
ATG use	26 (48%)	5 (6%)	31 (24%)
Clinical course			
Acute GVHD			
Grade 0–2	44	53	97
Grade 3–4	8	10	18
Chronic GVHD	15 (28%)	35 (45%)	50 (38%)
Infection	29 (53%)	48 (62%)	77 (58%)
Bacterial infection	11 (20%)	20 (26%)	31 (23%)
Fungal infection	4 (7%)	6 (8%)	10 (8%)
Viral infection	18 (33%)	35 (45%)	53 (40%)
Relapse	—	30 (39%)	—
Survival	51 (91%)	49 (64%)	100 (75%)

Abbreviations: ATG = antithymocyte globulin; CB = cord blood; MA = myeloablative; PID = primary immunodeficiency; RIC = reduced-intensity conditioning.

Tokyo Medical and Dental University and National Defense Medical College. Informed consent was obtained in accordance with the Declaration of Helsinki.

Measurement of TREC and KREC levels

TREC, sjKREC and cjKREC levels were measured by real-time PCR as described previously[15–19] at 1, 3 and 6 months, and yearly after HCT. RNase P was used as an internal control. Primer and probe sequences are listed in Supplementary Table I. The minimum detectable limit was 10 copies/μg DNA. TRECs or KRECs < 10 copies/μg DNA were defined as negative, and TREC or KREC levels of > 10 copies/μg DNA were defined as positive.

Monitoring of infections

Genomic DNA of eight human herpes virus species, BK virus, JC virus and parvovirus B19 in peripheral blood was measured by multiplex PCR and real-time PCR as described previously.[20] Adenovirus, hepatitis A virus, hepatitis B virus, hepatitis E virus, Norwalk-like virus, Coxsackie virus, ECHO virus, enterovirus, human metapneumovirus and human bocavirus were measured by real-time PCR as described elsewhere.[21] The minimum detectable limit was at least 30 copies/μg DNA.

Definitions

Patients treated with a > 5 Gy single dose of TBI, > 8 Gy fractionated TBI or > 8 mg/kg body weight of BU in addition to other cytoreduction agents were categorized as receiving myeloablative (MA) regimens.[22] HLA typing was performed by genotyping for HLA-A, B and DRB1 loci. GVHD was graded according to standard criteria.[23] We defined the incidence of infection as having symptoms of infection with detectable pathogens and severity ⩾ grade 3 as defined in the Common Terminology Criteria for Adverse Event (CTCAE) version 4.0, National Institutes of Health and National Cancer Institute.

Statistical analysis

Recipient age, recipient sex, disease, conditioning regimen, donor age, cell source, HLA disparity, relationship, acute GVHD, chronic GVHD, and the use of steroids or antithymocyte globulin (ATG) were chosen as clinical parameters. We categorized the diseases of enrolled patients as PID or malignancy. A MA regime was evaluated in comparison with reduced-intensity conditioning regimens and minimal conditioning regimens. HLA-mismatched HCT was compared with 6/6 HLA-matched HCT. Acute GVHD was graded as 0–4 and divided into two groups (0–2 and 3–4). The proportion of surviving patients was estimated by the Kaplan–Meier method and compared using the log-rank test. Factors that were found to be significant ($P < 0.05$) in univariate analysis were included in the multivariate analysis. Multivariate analyses of factors contributing to better TREC/KREC recovery were performed by excluding or including acute and chronic GVHD, steroid use, and ATG use, because these factors are post-HCT events and associated with other factors. Donor age was also excluded because it is restricted for BMT.

RESULTS

Levels of sjKRECs and cjKRECs recover faster than those of TRECs

First, we evaluated the recovery of TREC, sjKREC and cjKREC levels post transplantation.

One month after HCT, TRECs, sjKRECs and cjKRECs were detectable in 17 (17.5%), 34 (35.1%),and 28 (28.9%) of 97 patients, respectively. The median copy number was low (< 10 copies/μg DNA) in all assays (Figures 1a and b).

Eighty-two patients were examined 3 months after HCT. TRECs were positive in 15 (18.3%) patients, whereas sjKRECs and cjKRECs were positive in 57 (69.5%) and 59 (72.0%) patients, respectively (Figures 1c and d).

TRECs became positive in 41.3% of patients at 6 months and in 66.7% of patients 1 year post HCT. SjKRECs and cjKRECs were positive in 77.8% of patients at 6 months and in > 90% of patients at 1 year post HCT. The median level of TRECs was < 10 copies/μg DNA at 6 months and reached up to 1270 copies/μg DNA at 1 year. Interestingly, sjKRECs continued to increase for at least 1 year, while cjKRECs peaked at 6 months, and then started to decline (Figures 1e–h).

The recovery of sjKREC and cjKREC levels correlated as shown in Figures 1b, d, f, and h. This finding indicates that B-cell maturation is intact once B-cell engraftment is achieved. On the other hand, a considerable number of patients exhibited B-cell neogenesis in the absence of T-cell neogenesis, especially at the early stage post HCT (Figures 1a, c, and e).

We examined the trend of TRECs and KRECs in individual patients, of whom 71% had positive sjKRECs at 1 month and showed increased sjKRECs at 3 months. Similarly, the levels of sjKRECs detectable at 1 month increased at 6 months in 80% of the patients (Figure 2b). On the other hand, positive TRECs at 1 month did not indicate further T-cell recovery at a later period. When we examined patients with positive TRECs at 3 months, 10 of the 11 patients had increased TREC levels at 6 months, suggesting that positive TRECs at 3 months may serve as a predictor of T-cell reconstitution after 6 months (Figure 2a).

Longitudinal analysis showed that the recovery course of TRECs from 1 month to 15 years post HCT is at least not inferior to CBT when compared with that of BMT and PBSCT. Compared to BMT,

© 2014 Macmillan Publishers Limited

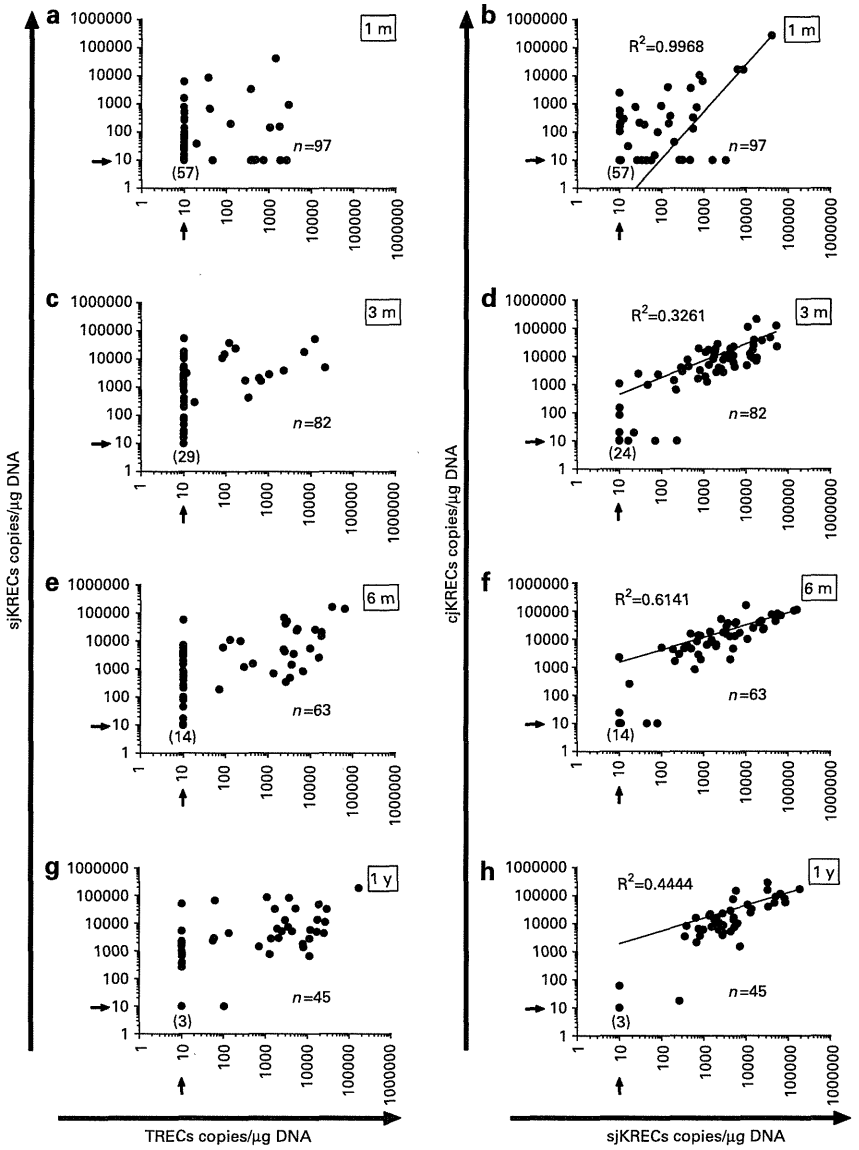

Figure 1. Recovery of TREC and KREC levels. Recovery of the levels of TRECs and sjKRECs, and sjKRECs and cjKRECs at 1 month (**a**, **b**), 3 months (**c**, **d**), 6 months (**e**, **f**) and 1 year (**g**, **h**) after HCT. Arrows show the detectable limit of the real-time PCR (10 copies/μg DNA). Values under the limit are considered 'negative'. Numbers in parentheses indicate the number of subjects who show a negative value (< 10 copies/μg DNA) for the indicated products.

KREC levels recovered more rapidly after CBT (Supplementary Figures 1 and 2). Final sjKREC/cjKREC levels reached the levels of the age-matched control when KRECs were fully recovered (data not shown).

Younger recipient age and CB favor increased levels of sjKRECs and cjKRECs

Next, we evaluated the factors that contributed to the levels of TRECs, sjKRECs and cjKRECs by regression analysis, including the factors listed in Materials and Methods (Supplementary Table II). A younger recipient and donor age was defined as < 18 years old.

In univariate analysis, a younger recipient age was a favorable factor for increased levels of TRECs, sjKRECs or cjKRECs post HCT. In fact, only the cjKREC levels of older recipients became close to those of younger recipients at 2 years after HCT (Figure 3). In BMT recipients, a younger donor age was a favorable factor for increased levels of TRECs, sjKRECs and cjKRECs (Supplementary Table II and Supplementary Figure 3). Compared with BM or PB, the use of CB was a favorable factor for increased levels of sjKRECs and cjKRECs after HCT (Figure 4 and Supplementary Table II).

A MA regime, PID, no or mild acute GVHD (grade 0–2), no chronic GVHD, no use of steroids, and no use of ATG were also favorable factors for increased levels of TRECs, sjKRECs or cjKRECs at various time points after HCT (Supplementary Table II).

On the basis of the results obtained from the univariate analysis, the following factors were used in multivariate analysis: recipient age, disease, conditioning regimen, cell source and relationship. Our results concerning TRECs largely reconfirmed previous reports,[13,24] indicating that a younger recipient age, no ATG use and a MA regime are associated with better TREC recovery. When focusing on B-cell recovery, we found that a younger recipient age was a favorable factor for increased levels of sjKRECs at 6 months to 2 years and cjKRECs at 6 months to 1 year after HCT. In addition, compared with BMT, CBT favored increased levels of sjKRECs at 1, 3 and 48 months. A MA regime was a favorable factor for increased levels of sjKRECs at 3 to 6 months (Table 2).

© 2014 Macmillan Publishers Limited

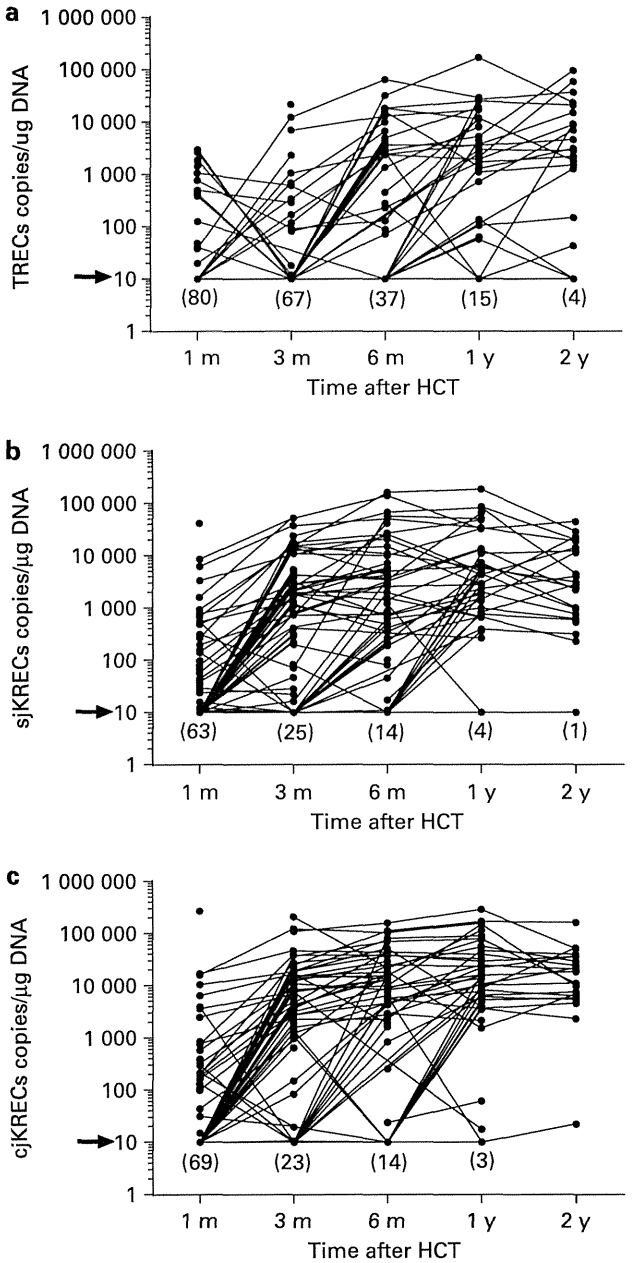

Figure 2. Levels of TRECs and KRECs after HCT. The levels of TRECs (**a**), sjKRECs (**b**) and cjKRECs (**c**) after HCT. The arrows show the detectable limit of the real-time PCR (10 copies/µg DNA). Values under this limit are considered 'negative'. Numbers in parentheses indicate the number of subjects who show a negative value (< 10 copies/µg DNA) for the indicated products.

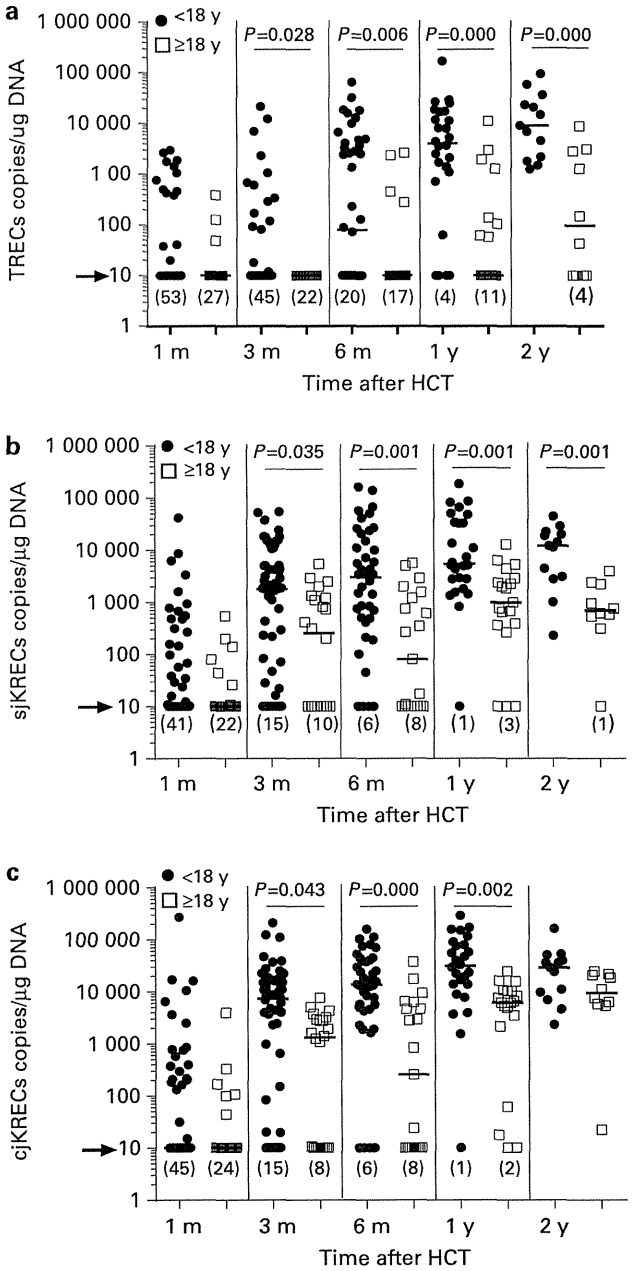

Figure 3. Recipient age and the levels of TRECs and KRECs. Recipient age and the levels of TRECs (**a**), sjKRECs (**b**) and cjKRECs (**c**). Closed circles indicate < 18 years old, and open squares indicate ⩾ 18 years old. Arrows show the detectable limit of the real-time PCR (10 copies/µg DNA). Values under this limit are considered 'negative'. Numbers in parentheses indicate the number of subjects who show a negative value (< 10 copies/µg DNA) for the indicated products.

By including acute GVHD, steroid use and ATG use in the analysis, grade 0–2 acute GVHD, no steroid use and no ATG use were identified as factors favoring better KREC recovery at various time points (Supplementary Table III). The analysis further including chronic GVHD suggested that the condition does not affect B-cell neoproduction (Supplementary Table IV).

We then performed multivariate analysis of a group of patients with malignancy. Compared with BM recipients, the results showed that sjKRECs and cjKRECs were more frequently detectable in CB recipients at 3 months (Supplementary Table V). Compared with BM recipients, in adult patients of ⩾18 years of age ($n=44$), the use of CB was a favorable factor for increased levels of sjKRECs at 1 month (Supplementary Table VI). These data show that CB use contributes to early recovery of neogenesis. In contrast, we observed no significant difference of T-cell recovery in adult patients when CB use was compared with BM at any time point after HCT (Supplementary Figure 4).

Positivity for sjKRECs 1 month after HCT is associated with decreased infectious episodes

We next investigated whether the levels of TRECs, sjKRECs or cjKRECs were associated with the occurrence of infections. We found that positive sjKRECs or TRECs 1 month after HCT correlated

© 2014 Macmillan Publishers Limited

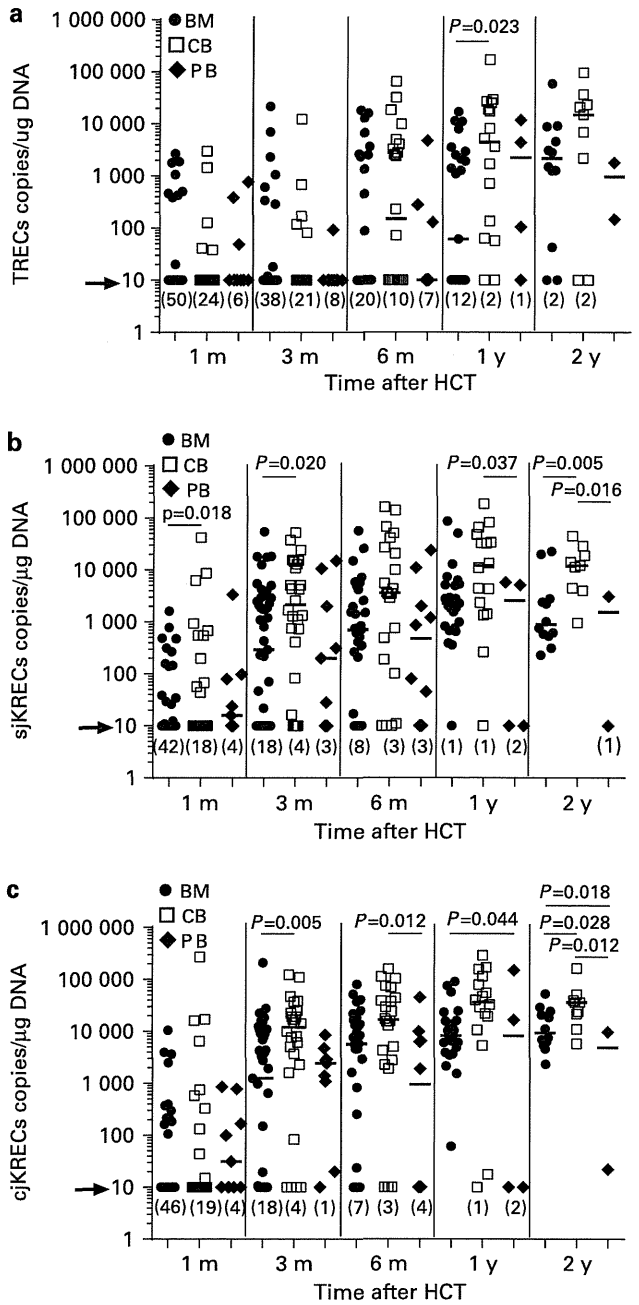

Figure 4. Cell source and the levels of TRECs and KRECs. Cell source and the levels of TRECs (**a**), sjKRECs (**b**) and cjKRECs (**c**). Closed circles indicate BM, open squares indicate cord blood and closed diamonds indicate peripheral blood. Arrows show the detectable limit of the real-time PCR (10 copies/μg DNA). Values under the limit are considered 'negative'. Numbers in parentheses indicate the number of subjects who show a negative value (< 10 copies/μg DNA) for the indicated products.

with decreased infectious episodes (Figure 5). Sixteen out of 34 patients who were positive for sjKRECs suffered from infections, whereas 43 of 63 patients who were negative for sjKRECs acquired infections (Figure 5b, $P = 0.033$).

We also examined the association between each index and the incidence of infectious episodes caused by bacteria, fungi or viruses. Although there was a tendency toward less bacterial infections in sjKREC- or cjKREC-positive groups, we found no statistical significance. Cumulative incidence of each infection did

Table 2. Multivariate analysis of factors that contributed to the levels of TRECs, sjKRECs and cjKRECs

Factors	*1 month*		*3 months*		*6 months*		*1 year*		*2 years*	
	β (95% CI)	*P-value*	*β (95% CI)*	*P-value*	*β (95% CI)*	*P-value*	*β (95% CI)*	*P-value*	*β (95% CI)*	*P-value*
TRECs										
Younger recipient age	0.084 (−0.213 to 0.449)	0.481	0.140 (−0.161 to 0.633)	0.241	0.231 (−0.133 to 1.400)	0.104	**0.379 (0.263 to 1.829)**	**0.010**[a]	**0.629 (0.662 to 2.511)**	**0.002**[a]
PID	0.217 (−0.077 to 0.665)	0.119	0.120 (−0.221 to 0.583)	0.373	0.126 (−0.505 to 1.158)	0.435	**0.348 (0.155 to 1.769)**	**0.021**[a]	0.355 (−0.254 to 2.118)	0.115
MA	**0.354 (0.137 to 0.853)**	**0.007**[a]	0.166 (−0.134 to 0.648)	0.194	0.049 (−0.635 to 0.893)	0.737	0.154 (−0.338 to 1.180)	0.269	−0.117 (−1.217 to 0.632)	0.512
BM (compared with CB)	0.088 (−0.194 to 0.428)	0.456	−0.071 (−0.488 to 0.275)	0.580	−0.183 (−1.241 to 0.296)	0.223	−0.256 (−1.514 to 0.111)	0.088	−0.018 (−0.925 to 0.837)	0.916
PB (compared with CB)	0.223 (−0.114 to 1.113)	0.109	−0.254 (−1.338 to 0.130)	0.105	−0.286 (−2.415 to 0.391)	0.154	−0.106 (−2.046 to 1.030)	0.508	0.033 (−1.742 to 2.032)	0.873
Relation	−0.075 (−0.491 to 0.272)	0.571	**0.344 (0.115 to 1.000)**	**0.014**[a]	0.220 (−0.345 to 1.568)	0.206	0.195 (−0.312 to 1.487)	0.194	0.116 (−0.735 to 1.367)	0.532
sjKRECs										
Younger recipient age	0.070 (−0.282 to 0.552)	0.553	0.072 (−0.427 to 0.841)	0.517	**0.339 (0.241 to 1.618)**	**0.009**[a]	**0.328 (0.060 to 1.292)**	**0.032**[a]	**0.414 (0.071 to 1.333)**	**0.031**[a]
PID	0.160 (−0.187 to 0.715)	0.248	0.178 (−0.186 to 1.098)	0.161	−0.053 (−0.883 to 0.610)	0.716	0.236 (−0.147 to 1.123)	0.128	0.282 (−0.310 to 1.308)	0.210
MA	0.167 (−0.151 to 0.719)	0.198	**0.263 (0.069 to 1.318)**	**0.030**[a]	**0.299 (0.098 to 1.471)**	**0.026**[a]	0.107 (−0.378 to 0.817)	0.462	0.069 (−0.514 to 0.747)	0.701
BM (compared with CB)	**−0.258 (−0.796 to −0.041)**	**0.030**[b]	**−0.372 (−1.566 to −0.347)**	**0.003**[b]	−0.230 (−1.284 to 0.095)	0.090	−0.181 (−1.010 to 0.268)	0.247	**−0.370 (−1.224 to −0.022)**	**0.043**[b]
PB (compared with CB)	−0.098 (−1.012 to 0.479)	0.479	**−0.407 (−2.824 to −0.480)**	**0.006**[b]	−0.349 (−2.495 to 0.025)	0.055	**−0.447 (−2.809 to 0.389)**	**0.011**[b]	−0.420 (−2.540 to 0.034)	0.056
Relation	0.149 (−0.200 to 0.727)	0.262	**0.394 (0.381 to 1.793)**	**0.003**[a]	0.194 (−0.320 to 1.398)	0.214	0.218 (−0.219 to 1.197)	0.170	−0.019 (−0.751 to 0.682)	0.920
cjKRECs										
Younger recipient age	0.017 (−0.450 to 0.519)	0.887	0.085 (−0.429 to 0.967)	0.445	**0.352 (0.309 to 1.822)**	**0.007**[a]	**0.383 (0.144 to 1.563)**	**0.020**[a]	0.171 (−0.375 to 0.869)	0.412
PID	**0.287 (0.024 to 1.112)**	**0.041**[a]	0.148 (−0.285 to 1.128)	0.239	−0.052 (−0.969 to 0.671)	0.717	0.145 (−0.407 to 1.055)	0.376	0.305 (−0.339 to 1.257)	0.240
MA	0.216 (−0.083 to 0.966)	0.098	**0.281 (0.136 to 1.510)**	**0.020**[a]	0.257 (−0.007 to 1.500)	0.052	0.015 (−0.654 to 0.721)	0.921	0.071 (−0.520 to 0.724)	0.733
BM (compared with CB)	−0.164 (−0.775 to 0.135)	0.166	**−0.427 (−1.890 to −0.548)**	**0.001**[b]	−0.189 (−1.297 to 0.219)	0.160	−0.033 (−0.810 to 0.662)	0.840	−0.261 (−0.967 to 0.218)	0.199
PB (compared with CB)	−0.026 (−0.985 to 0.812)	0.849	**−0.329 (−2.770 to −0.190)**	**0.025**[b]	**−0.422 (−3.035 to −0.267)**	**0.020**[b]	−0.346 (−2.730 to 0.056)	0.059	**−0.580 (−2.747 to −0.208)**	**0.025**[b]
Relation	0.158 (−0.225 to 0.893)	0.238	**0.336 (0.253 to 1.808)**	**0.010**[a]	0.160 (−0.454 to 1.433)	0.303	0.154 (−0.441 to 1.188)	0.359	0.001 (−0.706 to 0.708)	0.998

Abbreviations: CB = cord blood; cjKREC = coding joint kappa-deleting recombination excision circle; MA = myeloablative; PB = peripheral blood; PID = primary immunodeficiency; sjKREC = signal joint kappa-deleting recombination excision circle; TREC = T-cell receptor excision circle. Bold letters indicate significant factors. [a]Significant favorable factors that contributed to the levels of TRECs, sjKRECs and cjKRECs. [b]Significant unfavorable factors that contributed to the levels of TRECs, sjKRECs and cjKRECs.

© 2014 Macmillan Publishers Limited

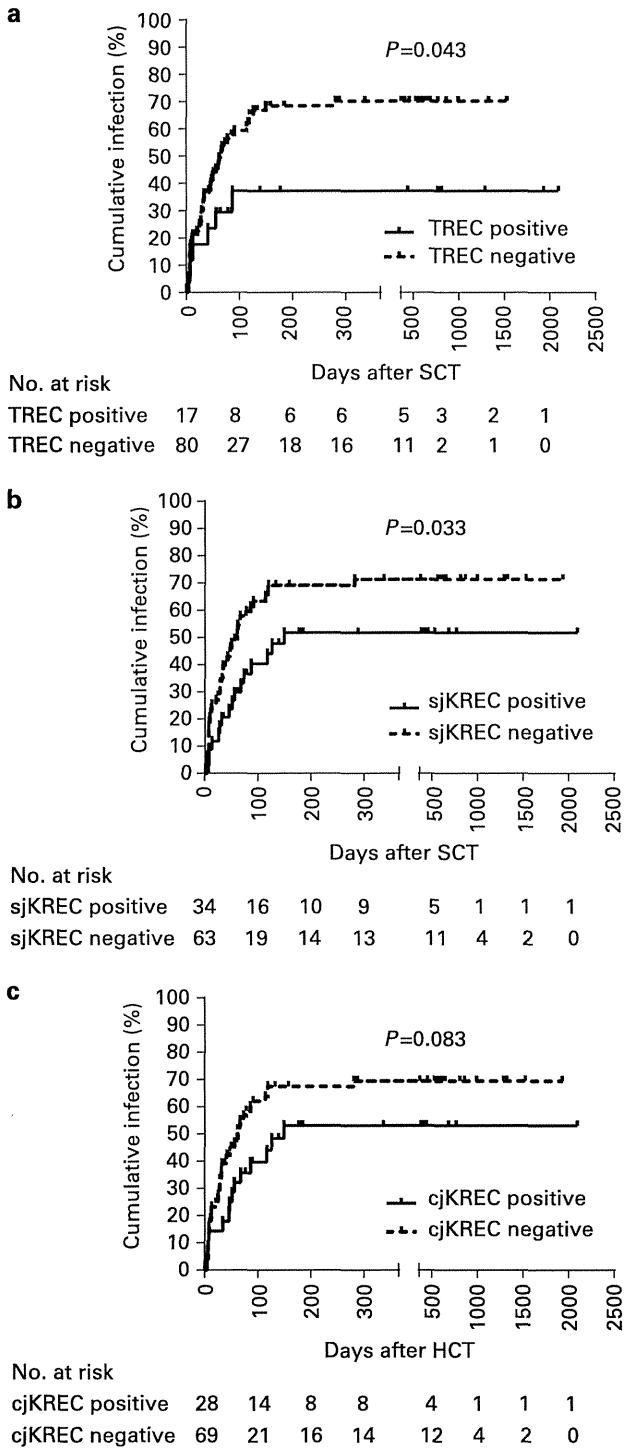

Figure 5. Cumulative incidence of infection after HCT. Cumulative incidence of infection and the levels of TRECs (**a**), sjKRECs (**b**) and cjKRECs (**c**) 1 month after HCT. Solid lines indicate the positive levels of TRECs (**a**), sjKRECs (**b**) and cjKRECs (**c**), and the dotted lines indicate their negative levels.

not correlate with negative TRECs, sjKRECs or cjKRECs at 3 months after HCT (data not shown).

DISCUSSION

In this study, we examined TRECs and sjKRECs/cjKRECs in post-transplantation patients with malignancies or PID. Our data showed the following. (1) The levels of sjKRECs and cjKRECs increase earlier than those of TRECs. (2) A younger recipient age is favorable for better recovery of sjKRECs and cjKRECs post HCT. (3) The use of CB achieves rapid recovery of sjKRECs and cjKRECs compared with that of BM or PB as a graft source. (4) Detectable sjKRECs 1 month after HCT is related to a decreased frequency of infectious episodes.

Patients with positive sjKRECs at 1 month had increased levels of sjKRECs at 3 and 6 months, suggesting that positivity can predict sound B-cell immune reconstitution. In addition, the levels of sjKRECs and cjKRECs increased earlier than those of TRECs (Figure 1, Supplementary Figures 1 and 2).

There have been no reports of the factors that contribute to better KREC reconstitution. Compared with BM and PB, we found that the levels of sjKRECs and cjKRECs recovered rapidly in patients who received CB. Faster B-cell reconstitution after CBT has been reported previously.[14,25] CB itself does not have high sjKREC/cjKREC levels. Our results suggest that rapid B-cell recovery by CBT is because of B-cell neogenesis and not B-cell expansion in the periphery.

A previous study has demonstrated that sjKREC levels are the highest in < 1-year-olds and then declines with age in healthy children.[17] Thus, it is likely that younger donors have an advantage in terms of B-cell reconstitution. Our results indicated that a younger recipient age also contributed to increased levels of sjKRECs and cjKRECs.

In addition, our data showed that acute 0–2 GVHD, no steroid use and no ATG use were associated with positive sjKRECs and cjKRECs (Supplementary Tables III and IV). These data indicate that steroid or ATG use affects not only T-cell recovery but also B-cell immune reconstitution.

As expected, patients with chronic GVHD showed significantly lower levels of TRECs at 6 months and 1 year. On the other hand, and in contrast to our expectation, we observed lower sjKRECs and cjKRECs from 3 months to 2 years in patients with chronic GVHD (Supplementary Figure 5). This observation does not support the data of Allen *et al.*,[26] which revealed increased numbers of B cells and expression of BAFF (B-cell-activating factor belonging to the TNF family) in patients with chronic GVHD. This discrepancy may be because the patients with chronic GVHD were on more active immunosuppressants compared with those without chronic GVHD. Additionally, there may be relatively high levels of KRECs in patients with the severe extensive type of chronic GVHD. However, we would need more patients and additional analyses of B-cell numbers and activation to reach a conclusion.

Our study suggests that patients with positivity for TRECs or sjKRECs at 1 month are less likely to develop post-transplant infections. The contribution of earlier B-cell recovery to overall immunity, especially anti-microbial immunity, needs further investigation. Patients with early B-cell neogenesis may attain early myeloid recovery. B-cells may also serve as antigen-presenting cells in addition to antibody-producing cells.

A correlation between KREC levels and prognosis has not been addressed previously. Although there was a tendency toward better survival for the KREC-positive group at 1 month, we observed no statistical significance. Further study with a larger cohort is required to determine whether the difference can be significant.

It is still unclear whether TREC levels are lower in patients post CBT than in those receiving BMT.[25] Our data focusing on adult patients showed that T-cell recovery was at least not inferior and appeared to be similar in CB and BM recipients (data not shown). On the other hand, compared with BM and PB, CB was superior for B-cell recovery. This observation suggests quantitative superiority of B-cell recovery following CBT. Further study should investigate the repertoire diversity and somatic hypermutation of B-cell receptors to evaluate qualitative differences and determine whether rapid qualitative maturation has an effect on improved

© 2014 Macmillan Publishers Limited

outcomes. In combination with *in vitro* immunological data and clinical data such as long-term infection, autoimmunity and immunological findings, KRECs and TRECs may serve as useful tools for immunological monitoring after HCT.

CONFLICT OF INTEREST

The authors declare no conflict of interest.

ACKNOWLEDGEMENTS

This work was in part supported by Health and Labour Sciences Research Grants for Intractable diseases (H23-003 and H24-008 to TM, and H24-013 to KI).

REFERENCES

1 Gooley TA, Chien JW, Pergam SA, Hingorani S, Sorror ML, Boeckh M *et al.* Reduced mortality after allogeneic hematopoietic-cell transplantation. *N Engl J Med* 2010; **363**: 2091–2101.
2 Antoine C, Muller S, Cant A, Cavazzana-Calvo M, Veys P, Vossen J *et al.* Long-term survival and transplantation of haemopoietic stem cells for immunodeficiencies: report of the European experience 1968-99. *Lancet* 2003; **361**: 553–560.
3 Dvorak CC, Cowan MJ. Hematopoietic stem cell transplantation for primary immunodeficiency disease. *Bone Marrow Transplant* 2008; **41**: 119–126.
4 Gluckman E, Rocha V, Boyer-Chammard A, Locatelli F, Arcese W, Pasquini R *et al.* Outcome of cord-blood transplantation from related and unrelated donors. Eurocord Transplant Group and the European Blood and Marrow Transplantation Group. *N Engl J Med* 1997; **337**: 373–381.
5 Kurtzberg J, Laughlin M, Graham ML, Smith C, Olson JF, Halperin EC *et al.* Placental blood as a source of hematopoietic stem cells for transplantation into unrelated recipients. *N Engl J Med* 1996; **335**: 157–166.
6 Laughlin MJ, Eapen M, Rubinstein P, Wagner JE, Zhang MJ, Champlin RE *et al.* Outcomes after transplantation of cord blood or bone marrow from unrelated donors in adults with leukemia. *N Engl J Med* 2004; **351**: 2265–2275.
7 Rocha V, Labopin M, Sanz G, Arcese W, Schwerdtfeger R, Bosi A *et al.* Transplants of umbilical-cord blood or bone marrow from unrelated donors in adults with acute leukemia. *N Engl J Med* 2004; **351**: 2276–2285.
8 Wagner JE, Rosenthal J, Sweetman R, Shu XO, Davies SM, Ramsay NK *et al.* Successful transplantation of HLA-matched and HLA-mismatched umbilical cord blood from unrelated donors: analysis of engraftment and acute graft-versus-host disease. *Blood* 1996; **88**: 795–802.
9 Szabolcs P, Niedzwiecki D. Immune reconstitution in children after unrelated cord blood transplantation. *Biol Blood Marrow Transplant* 2008; **14**: 66–72.
10 Hazenberg MD, Verschuren MC, Hamann D, Miedema F, van Dongen JJ. T cell receptor excision circles as markers for recent thymic emigrants: basic aspects, technical approach, and guidelines for interpretation. *J Molec Med* 2001; **79**: 631–640.
11 Brown JA, Stevenson K, Kim HT, Cutler C, Ballen K, McDonough S *et al.* Clearance of CMV viremia and survival after double umbilical cord blood transplantation in adults depends on reconstitution of thymopoiesis. *Blood* 2010; **115**: 4111–4119.
12 Lewin SR, Heller G, Zhang L, Rodrigues E, Skulsky E, van den Brink MR *et al.* Direct evidence for new T-cell generation by patients after either T-cell-depleted or unmodified allogeneic hematopoietic stem cell transplantations. *Blood* 2002; **100**: 2235–2242.
13 Sairafi D, Mattsson J, Uhlin M, Uzunel M. Thymic function after allogeneic stem cell transplantation is dependent on graft source and predictive of long term survival. *Clin Immunol* 2012; **142**: 343–350.
14 Komanduri KV, St John LS, de Lima M, McMannis J, Rosinski S, McNiece I *et al.* Delayed immune reconstitution after cord blood transplantation is characterized by impaired thymopoiesis and late memory T-cell skewing. *Blood* 2007; **110**: 4543–4551.
15 van Zelm MC, Szczepanski T, van der Burg M, van Dongen JJ. Replication history of B lymphocytes reveals homeostatic proliferation and extensive antigen-induced B cell expansion. *J Exp Med* 2007; **204**: 645–655.
16 Hazenberg MD, Otto SA, Cohen Stuart JW, Verschuren MC, Borleffs JC, Boucher CA *et al.* Increased cell division but not thymic dysfunction rapidly affects the T-cell receptor excision circle content of the naive T cell population in HIV-1 infection. *Nat Med* 2000; **6**: 1036–1042.
17 Kamae C, Nakagawa N, Sato H, Honma K, Mitsuiki N, Ohara O *et al.* Common variable immunodeficiency classification by quantifying T-cell receptor and immunoglobulin kappa-deleting recombination excision circles. *J Allergy Clin Immunol* 2012; **131**: 1437–1440 e5.
18 Morinishi Y, Imai K, Nakagawa N, Sato H, Horiuchi K, Ohtsuka Y *et al.* Identification of severe combined immunodeficiency by T-cell receptor excision circles quantification using neonatal guthrie cards. *J Pediatr* 2009; **155**: 829–833.
19 Nakagawa N, Imai K, Kanegane H, Sato H, Yamada M, Kondoh K *et al.* Quantification of kappa-deleting recombination excision circles in Guthrie cards for the identification of early B-cell maturation defects. *J Allergy Clin Immunol* 2011; **128**: 223–225 e2.
20 Sugita S, Shimizu N, Watanabe K, Mizukami M, Morio T, Sugamoto Y *et al.* Use of multiplex PCR and real-time PCR to detect human herpes virus genome in ocular fluids of patients with uveitis. *Br J Ophthalmol* 2008; **92**: 928–932.
21 Ono A, Mochizuki M, Yamaguchi K, Miyata N, Watanabe T. Increased number of circulating HTLV-1 infected cells in peripheral blood mononuclear cells of HTLV-1 uveitis patients: a quantitative polymerase chain reaction study. *Br J Ophthalmol* 1995; **79**: 270–276.
22 Bacigalupo A, Ballen K, Rizzo D, Giralt S, Lazarus H, Ho V *et al.* Defining the intensity of conditioning regimens: working definitions. *Biol Blood Marrow Transplant* 2009; **15**: 1628–1633.
23 Przepiorka D, Weisdorf D, Martin P, Klingemann HG, Beatty P, Hows J *et al.* 1994 Consensus Conference on Acute GVHD Grading. *Bone Marrow Transplant* 1995; **15**: 825–828.
24 Clave E, Busson M, Douay C, Peffault de Latour R, Berrou J, Rabian C *et al.* Acute graft-versus-host disease transiently impairs thymic output in young patients after allogeneic hematopoietic stem cell transplantation. *Blood* 2009; **113**: 6477–6484.
25 Bartelink IH, Belitser SV, Knibbe CA, Danhof M, de Pagter PJ, Egberts AC *et al.* Immune reconstitution kinetics as an early predictor for mortality using various hematopoietic stem cell sources in children. *Biol Blood Marrow Transplant* 2012; **19**: 305–313.
26 Allen JL, Fore MS, Wooten J, Roehrs PA, Bhuiya NS, Hoffert T *et al.* B cells from patients with chronic GVHD are activated and primed for survival via BAFF-mediated pathways. *Blood* 2012; **120**: 2529–2536.

Supplementary Information accompanies this paper on Bone Marrow Transplantation website (http://www.nature.com/bmt)

© 2014 Macmillan Publishers Limited

Gastroenterology 2015;148:565–578

BASIC AND TRANSLATIONAL—ALIMENTARY TRACT

Inhibition of Plasmin Protects Against Colitis in Mice by Suppressing Matrix Metalloproteinase 9–Mediated Cytokine Release From Myeloid Cells

Shinya Munakata,[1,2,3,*] **Yoshihiko Tashiro,**[1,2,3,*] Chiemi Nishida,[1,3] Aki Sato,[1] Hiromitsu Komiyama,[1,2] Hiroshi Shimazu,[1] Douaa Dhahri,[3] Yousef Salama,[3] Salita Eiamboonsert,[3] Kazuyoshi Takeda,[4] Hideo Yagita,[4] Yuko Tsuda,[5] Yoshio Okada,[5] Hiromitsu Nakauchi,[1] Kazuhiro Sakamoto,[2] Beate Heissig,[1,3,6,§] and Koichi Hattori[1,6,§]

[1]*Stem Cell Regulation,* [3]*Stem Cell Dynamics, Center for Stem Cell Biology and Regenerative Medicine, Institute of Medical Science at the University of Tokyo, Minato-ku, Tokyo, Japan;* [2]*Department of Coloproctological Surgery,* [4]*Department of Immunology,* [6]*Atopy (Allergy) Center, Juntendo University School of Medicine, Bunkyo-ku, Tokyo, Japan;* [5]*Faculty of Pharmaceutical Sciences, Kobe Gakuin University, Ikawadani-cho, Nishi-ku, Kobe, Japan*

BACKGROUND & AIMS: Activated proteases such as plasmin and matrix metalloproteinases (MMPs) are activated in intestinal tissues of patients with active inflammatory bowel diseases. We investigated the effect of plasmin on the progression of acute colitis. **METHODS:** Colitis was induced in *Mmp9*$^{-/-}$, *Plg*$^{-/-}$, and C57BL/6 (control) mice by the administration of dextran sulfate sodium, trinitrobenzene sulfonic acid, or CD40 antibody. Plasmin was inhibited in control mice by intraperitoneal injection of YO-2, which blocks its active site. Mucosal and blood samples were collected and analyzed by reverse-transcription polymerase chain reaction and immunohistochemical analyses, as well as for mucosal inflammation and levels of cytokines and chemokines. **RESULTS:** Circulating levels of plasmin were increased in mice with colitis, compared with controls. Colitis did not develop in control mice injected with YO-2 or in *Plg*$^{-/-}$ mice. Colons from these mice had reduced infiltration of Gr1+ neutrophils and F4/80+ macrophages, and reduced levels of inflammatory cytokines and chemokines. Colonic inflammation and colitis induction required activation of endogenous MMP9. After colitis induction, mice given YO-2, *Plg*$^{-/-}$ mice, and *Mmp9*$^{-/-}$ mice had reduced serum levels of tumor necrosis factor and C-X-C motif chemokine ligand 5, compared with control mice. **CONCLUSIONS:** In mice, plasmin induces a feedback mechanism in which activation of the fibrinolytic system promotes the development of colitis via activation of MMP9 or proteolytic enzymes. The proteolytic environment stimulates the influx of myeloid cells into the colonic epithelium and the production of tumor necrosis factor and C-X-C motif chemokine ligand 5. In turn, myeloid CD11b+ cells release the urokinase plasminogen activator, which accelerates plasmin production. Disruption of the plasmin-induced chronic inflammatory circuit therefore might be a strategy for colitis treatment.

Keywords: IBD; Mouse Model; Plasminogen; UC.

Crohn's disease and ulcerative colitis, the major forms of inflammatory bowel disease (IBD) in human beings, result from the interaction of genetic and environmental factors that ultimately promote an immunopathologic process leading to chronic inflammation.[1] Treatment of IBD generally relieves symptoms, but is not curative. Activation of proteases such as matrix metalloproteinases (MMPs), or serine proteases, such as plasmin, can break down the intestinal-epithelial barrier because of their potential to degrade components of the extracellular matrix, resulting in the invasion of inflammatory cells.[2]

MMP9, expressed by epithelial cells, plays an important role in the development of colitis by modulating cell-matrix interaction and wound healing.[3] MMP inhibitor treatment is effective for colitis, but patients have described side effects including severe lethargy and chills. Therefore, the therapeutic effects of more selective inhibitors of disease-associated MMPs currently are under investigation.[4] Another way of controlling the activation of MMPs is through the serine protease plasmin,[5–7] which has been shown to be important for the release of cytokines/chemokines such as Kit ligand, monocyte chemoattractant protein-1, C-X-C motif chemokine ligand 5 (CXCL5), and basic fibroblastic growth factor.[7–11] It is conceivable that the production of proinflammatory cytokines such as tumor necrosis factor α (TNF-α) also is regulated via plasmin-mediated MMP activation. TNF-α is induced rapidly in the intestinal mucosa during the initial activation of immune cells, and this induction is linked to disease progression during IBD.[12]

*Authors share co-first authorship; §Authors share co-senior authorship.

Abbreviations used in this paper: **Ab, antibody; CXCL5, C-X-C motif chemokine ligand 5; DAI, disease activity index; DSS, dextran sulfate sodium; FDP, fibrin degradation product; IBD, inflammatory bowel disease; IL, interleukin; MMP, matrix metalloproteinase; PA, plasminogen activator; PAP, plasmin-antiplasmin complex; Plg, plasminogen; TNBS, trinitrobenzene sulfonic acid; TNF, tumor necrosis factor; uPA/*Plau*, urokinase-type plasminogen activator; YO-2, *trans*-4-aminomethylcyclohexanecarbonyl-Tyr(*O*-Pic)-octylamide.**

© 2015 by the AGA Institute
0016-5085/$36.00
http://dx.doi.org/10.1053/j.gastro.2014.12.001

Plasmin, a key enzyme of the fibrinolytic cascade, can degrade the fibrin clot. It is generated by conversion from its precursor, plasminogen (Plg), by the plasminogen activators (PAs) tissue-type PA (*Plat*), and urokinase-type PA (uPA/*Plau*). Early clinical studies showed that circulating monocytes derived from IBD patients showed increased secretion of PA,[13] and that disease activity depended on up-regulation of uPA in the active stage of the disease.[14]

In the present study, we examined the role of the fibrinolytic system in patients with IBD. We show that genetic and pharmacologic plasmin inhibition prevents the progression of IBD in experimental models of colitis, and ameliorates the disease in part by suppressing the MMP9-dependent influx of inflammatory cells and production of inflammatory cytokines.

Materials and Methods

Animal Studies

Mmp9$^{+/+}$ and *Mmp9*$^{-/-}$ mice and *Plg*$^{+/+}$ and *Plg*$^{-/-}$ mice each were used after 10 back-crosses onto a C57BL/6 background. C57BL/6 recombinase-activating gene 2 (Rag2$^{-/-}$) mice were obtained from the Central Institute for Experimental Animals (Kawasaki, Japan). Animal studies were approved by the Animal Review Board of Juntendo University (Tokyo, Japan).

Induction of Colitis

Experimental dextran sulfate sodium (DSS) (ICN Biomedical molecular weight, 36,000–50,000 daltons; ICN Biomedicals Inc, Ohio, GA) colitis was induced by administering 2% DSS via drinking water on days 0–7. Trinitrobenzene sulfonic acid (TNBS)-induced colitis was induced by colonic injection of 100 μL

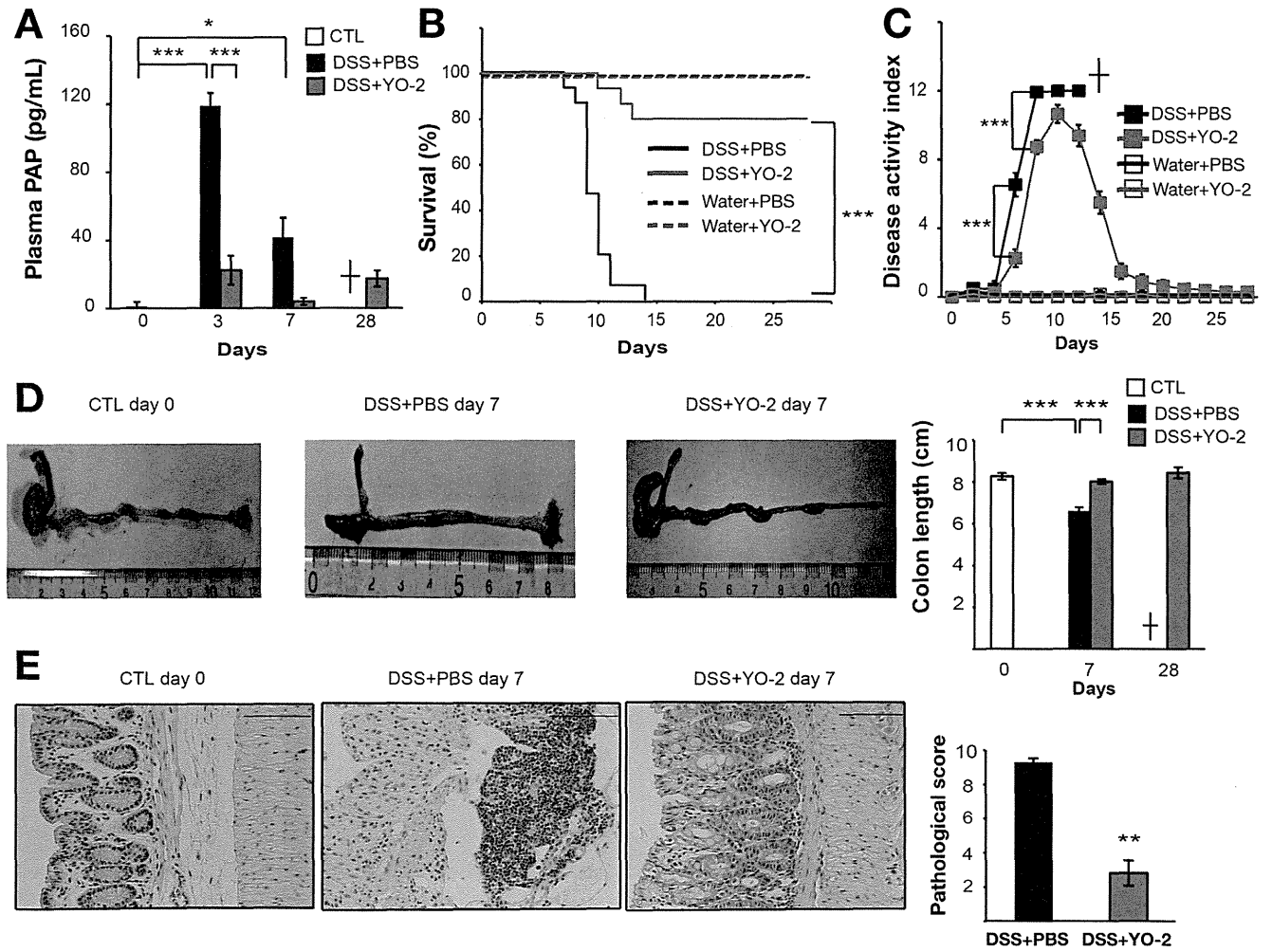

Figure 1. Plasmin inhibition prevents DSS-induced colitis progression. Colitis was induced by DSS and mice were injected with or without YO-2. (*A*) Plasma derived from mice treated with or without YO-2 was analyzed for PAP as a measure of active plasmin by enzyme-linked immunosorbent assay. n = 3/group. (*B*) Percentage survival and (*C*) DAI were determined at the indicated time points in the following treatment groups: 2% DSS + phosphate-buffered saline (PBS), n = 15; 2% DSS + YO-2, n = 15; water + PBS and water + YO-2, n = 5. (*D*) Colon lengths were measured at the indicated time points. n = 9–14/group. (*E*) Representative H&E-stained colon sections are shown. *Scale bars*: 200 μm. Histologic inflammatory scores were determined for each section from DSS-induced mice treated with/without YO-2. n = 3/group. Values represent means ± SEM. *$P < .05$, **$P < .01$, and ***$P < .001$, determined by a 2-tailed Student *t* test and log-rank test.

of 2.5% TNBS (Sigma, St. Louis, MO) dissolved in 50% ethanol. The control group received only 50% ethanol. Anti-CD40 antibody (Ab) (clone FGK45; kindly provided by Dr Yagita, Department of Immunology, Juntendo University School of Medicine).[15,16]

Trans-4-aminomethylcyclohexanecarbonyl-Tyr(*O*-Pic)-octylamide (YO-2)[17] (kindly provided by Yoshio Okada, The Faculty of Pharmaceutical Science, Kobe Gakuin University) was administered by intraperitoneal injection, once per day at 4 mg/kg/day from days 0 to 28. The tranexamic acid moiety of YO-2 interacts with the active center of plasmin. The MMP inhibitor (N-hydroxy-2-[(4-methoxysulfonyl)(3-picolyl)-amino]-3-methylbutanamide [MMI270]) (Novartis Pharma Corporation, Basel, Switzerland)[18] was administered orally at a dose of 100 mg/kg/day from days 0 to 7.

CD11b neutralizing antibody treatment. Mice were injected with 500 μg/mouse of anti-CD11b antibody (Ab) (clone 5C6; kindly provided by Dr Yagita, Juntendo University) or control IgG on days 0, 2, and 4. The clinical scoring of the disease activity index (DAI) for DSS-induced colitis was based on weight loss, stool consistency, and bleeding, as described previously by Cooper et al.[19]

Histology

Colon sections were stained with H&E and Elastica van Gieson staining. Histologic scoring was performed as described by Cooper et al.[19]

Bleeding Time

The mouse's tail was warmed to 37°C, and amputated 1 cm from the tail tip. Blood was blotted onto filter paper every 15 seconds.

Immunohistochemistry

Colon sections were stained with the anti-Gr1 Ab (clone RB6-8C5; R&D Systems, Minneapolis, MN), anti-MMP9 Ab (R&D Systems), anti-F4/80 Ab (clone A3-1; AbD Serotec, Oxford, United Kingdom), biotin-conjugated anti-CD11b Ab (clone M1-70; BD Pharmingen, San Diego, CA), anti-uPA Ab (Proteintech, Chicago,

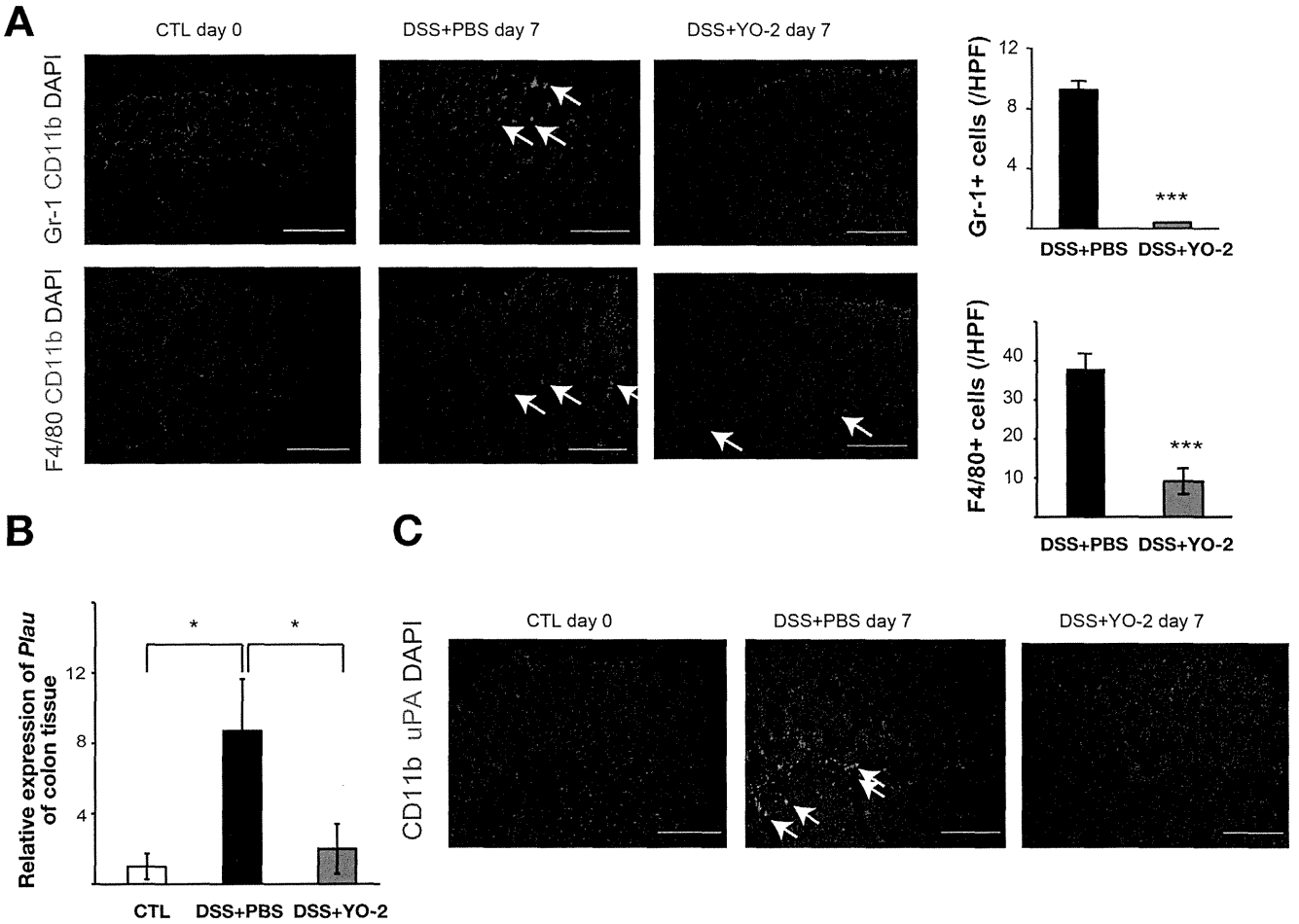

Figure 2. Plasmin inhibition suppresses the influx of myeloid cells into colonic tissue. (*A*) Representative immunohistochemical images of Gr-1/CD11b- and F4/80/CD11b-stained colon sections retrieved 7 days after DSS induction of C57BL/6 mice treated with or without YO-2. *Arrows* indicate positively stained cells. n = 3/group. *Scale bars*: 200 μm. *Right*: Indicated cell populations were quantified per high-power field (HPF). (*B*) *Plau* gene expression in colon retrieved from mice treated with or without YO-2 was semiquantitated by polymerase chain reaction. Levels were normalized to *Actb*. n = 3/group. (*C*) Staining of colonic sections showed uPA staining of a CD11b$^+$ cell subpopulation. *Scale bars*: 200 μm. Data represent means ± SEM. *Arrows* indicate double positive cells n = 3 group. *$P < .05$ and ***$P < .001$, determined by a 2-tailed Student *t* test. DAPI, 4′,6-diamidino-2-phenylindole.